Table 1. *Heart weight, echocardiographic, and hemodynamic data on day 14*[a]

| | Sham ($n$ = 9) | MI-C ($n$ = 10) | MI-G ($n$ = 10) | MI-GM ($n$ = 10) |
|---|---|---|---|---|
| BW, g | 252 ± 13 | 254 ± 14 | 242 ± 11 | 242 ± 14 |
| RVW/BW, g/kg | 0.5 ± 0.03 | 0.8 ± 0.06* | 0.8 ± 0.05* | 0.9 ± 0.06* |
| LVW/BW, g/kg | 2.0 ± 0.04 | 2.1 ± 0.08 | 2.1 ± 0.08 | 2.1 ± 0.12 |
| LVEDD, mm | 6.2 ± 0.2 | 8.5 ± 0.2* | 8.1 ± 0.1*† | 9.0 ± 0.1*† |
| LVESD, mm | 3.7 ± 0.1 | 6.9 ± 0.1* | 6.1 ± 0.2*† | 7.6 ± 0.1*† |
| FS, % | 41 ± 1.9 | 19 ± 1.5* | 24 ± 1.1*† | 15 ± 0.7*† |
| LVSP, mmHg | 123 ± 3 | 101 ± 4* | 102 ± 2* | 110 ± 5* |
| LVEDP, mmHg | 3.4 ± 0.4 | 9.7 ± 0.6* | 8.0 ± 0.5*† | 12.3 ± 1.1*† |
| LV $+dP/dt_{max}$, mmHg/s | 9415 ± 441 | 4530 ± 195* | 5828 ± 227*† | 3608 ± 356*† |
| LV $-dP/dt_{min}$, mmHg/s | −7280 ± 830 | −3536 ± 242* | −3595 ± 159* | −3675 ± 220* |

[a] BW, body weight; RVW, right ventricular weight; LVW, left ventricular weight; LVEDD, left ventricular end-diastolic dimension; LVESD, left ventricular end-systolic dimension; FS, fractional shortening; LVSP, left ventricular systolic pressure; LVEDP, left ventricular end-diastolic pressure; LV $+dP/dt_{max}$, left ventricular maximum rate of isovolumic pressure development; LV $-dP/dt_{min}$, left ventricular minimum rate of isovolumic pressure decay. Values are means ± SEM. *, $p < 0.05$ vs. sham; †, $p < 0.05$ vs. MI-C.

plasmacytoid DC followed by proliferation of Th2 cells (24–26). Therefore, we hypothesized that G-CSF and GM-CSF diversely regulate DC maturation through modulation of the Th1/Th2 balance during infarct healing and affect postinfarction LV remodeling. To test this hypothesis, we examined the dynamics of DC in a rat MI model using OX62 Ab, which is a reliable marker for the

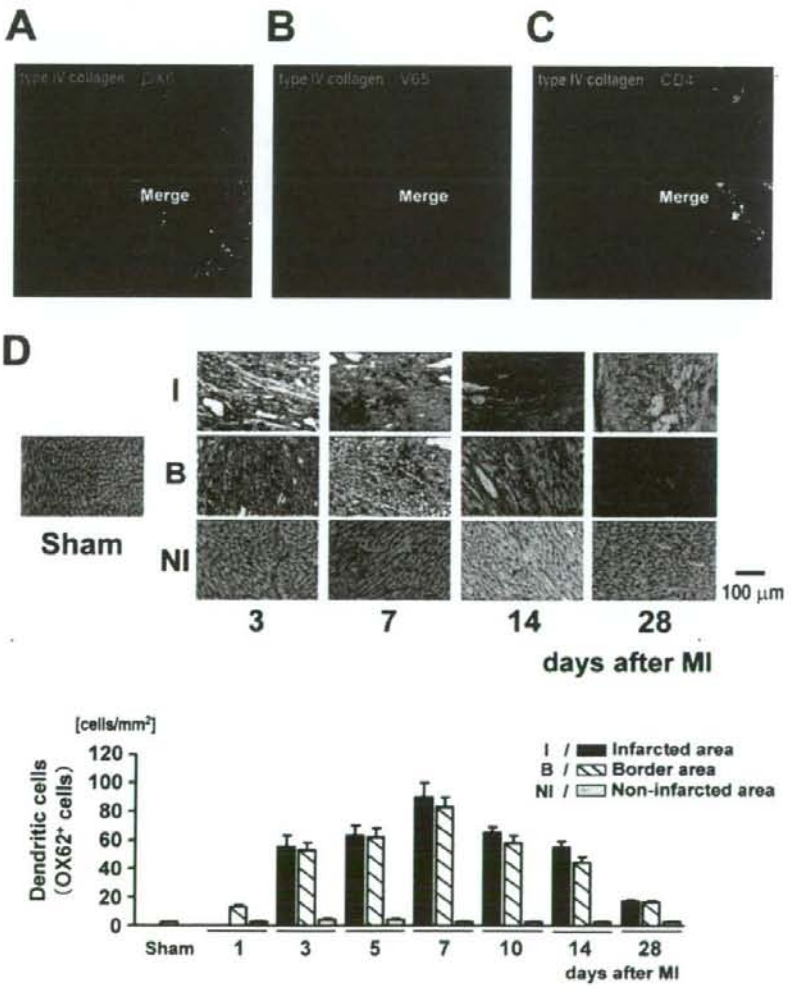


**FIGURE 1.** DC in infarcted heart. *A*, Triple immunofluorescent staining for OX62 (red), OX6 (green), and type IV collagen (blue). *B*, Triple immunofluorescent staining for OX62 (red), V65 (green), and type IV collagen (blue). *C*, Triple immunofluorescent staining for OX62 (red), CD4 (green), and type IV collagen (blue). All images in A–C are from myocardium of MI-C group on day 7. *D*, Immunohistochemical staining of myocardial sections to evaluate the time course changes in $OX62^+$ DC (blue) infiltration of infarcted (I), border (B), and noninfarcted (NI) areas ($n$ = 4/group). All specimens were stained for type IV collagen (brown) to show the tissue framework. Values are means ± SEM.

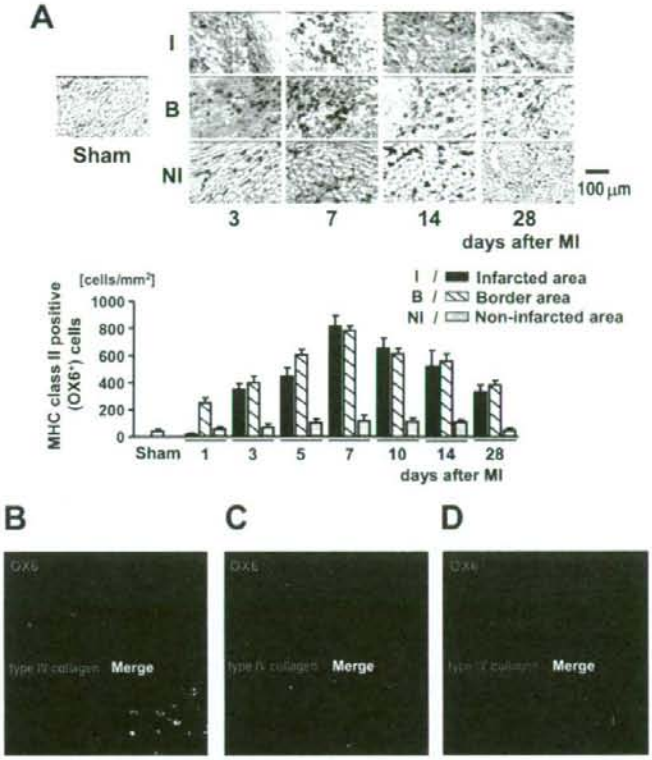


**FIGURE 2.** MHC class II$^+$ cells in myocardium. *A*, Immunohistochemical staining of myocardial sections using OX6 (blue) mAb to evaluate the time course changes in MHC class II$^+$ (OX6$^+$) cell infiltration of infarcted (I), border (B), and noninfarcted (NI) areas ($n$ = 4/group). All specimens were stained for type IV collagen (brown) to show the tissue framework. *B*, Triple immunofluorescent staining for OX6 (green), ED-1 (red), and type IV collagen (blue). *C*, Triple immunofluorescent staining for OX6 (green), ED-2 (red), and type IV collagen (blue). *D*, Triple immunofluorescent staining for OX6 (green), ED-3 (red), and type IV collagen (blue). Values are means ± SEM.

rat DC subpopulation (27), and clarified the effects of G-CSF and GM-CSF on DC infiltration and LV remodeling. Although resident DC in the rat heart are mostly negative for OX62, most infiltrating DC in a cardiac allograft model (28) and in a liver inflammation model (29) were shown to be OX62$^+$. Furthermore, we investigated the expression of HSP70 and TLRs to evaluate the triggers of DC activation and maturation, and IFN-γ, IL-4, and IL-10 as representative Th1 and Th2 cytokines in the infarcted heart.

## Materials and Methods

### *Animals and surgical procedure*

All procedures were performed in accordance with the Keio University animal care guidelines, which conform to the "Guide for the Care and Use of Laboratory Animals" (National Institutes of Health publication 85-23, revised 1996). Left ventricular MI was created in 9-wk-old male Wistar rats (Sankyo Laboratory Service) weighing 220–280 g, by left coronary artery ligation as previously described (22). Coronary ligation was performed in 166 rats. The same procedure was performed for sham-operated control animals ($n$ = 27) except that the ligature was left untied. The MI rats surviving the operation for 3 h ($n$ = 151) were randomly assigned to three groups: 1) recombinant human G-CSF (Kyowa Hakko Kogyo; 20 μg/kg/day) administered s.c. for 7 days (MI-G, $n$ = 45), (2) GM-CSF inducer (romurtide, 200 μg/kg/day) administered i.p. for 7 days (MI-GM, $n$ = 40), and (3) saline-treated controls (MI-C, $n$ = 66). Rats were housed under standardized conditions with free access to standard food and drinking water. A total of 116 rats (MI-G, $n$ = 33; MI-GM, $n$ = 28; MI-C, $n$ = 55) survived and were sacrificed 1, 3, 5, 7, 10, 14, and 28 days after surgery according to the study protocol.

### *Echocardiographic, hemodynamic, heart weight, and infarct size measurements*

Animals (sham-operated rats, $n$ = 9; MI-C, $n$ = 10; MI-G, $n$ = 10; MI-GM, $n$ = 10) were lightly anesthetized by i.p. administration of pentobarbital 2 wk after MI. Transthoracic echocardiography (8.5-MHz linear transducer; EnVisor C, Philips Medical Systems) and hemodynamic measurements using a miniature pressure transducer (SPC-320, Millar Instruments) were performed as previously described (22). The hearts were then excised and divided into left and right ventricles, and each ventricle was weighed separately. The investigators who conducted these procedures were blinded to the treatment of the animals. Infarct size was measured as the percentage of infarcted epicardium and endocardium of the LV, as previously described (22).

### *Antibodies and reagents*

For immunohistochemical analyses, mouse mAbs specific for rat determinants, including Abs against rat DC (OX62), MHC class II RT1B (OX6), CD4 (W3/25), γδ T cells (V65), CD68 (ED-1), CD163 (ED-2), ED-3, CD45, CD45R (His24), and CD86 (B7-2) were obtained from Serotec. An anti-BrdU mAb was purchased from Oxford Biotechnology. A rabbit anti-mouse type IV collagen polyclonal Ab to outline the tissue framework was purchased from LSL. As secondary Abs, an alkaline phosphatase (ALP)-labeled goat anti-mouse IgG (Sigma-Aldrich), a HRP-labeled anti-rabbit IgG (Cappel), and an ALP-labeled donkey anti-mouse IgG (Jackson ImmunoResearch Laboratories) were employed. For immunoblotting analyses, mouse anti-rat HSP70 mAb (Stress-Gen Biotechnologies) and rabbit polyclonal anti-rat TLR4 Ab (Santa Cruz Biotechnology) were used. As secondary Abs, an HRP-labeled anti-mouse IgG (Jackson ImmunoResearch Laboratories) and an HRP-labeled anti-rabbit IgG (Santa Cruz Biotechnology) were employed.

### *Immunohistochemical analyses*

Triple immunoenzymatic staining with mouse mAbs was performed as previously described (28). In brief, fresh cryosections were fixed in acetone for 10 min, air-dried, and rehydrated in PBS. Sections were fixed further with formol calcium solution (4% paraformaldehyde in 1% $CaCl_2$ (pH 7.0)) for 2 min and washed. As the first step, sections were incubated with the first mAbs for 1 h at room temperature and then with ALP-labeled anti-mouse IgG for 1 h at room temperature. After fixing in 1% glutaraldehyde for 30 s in PBS, the ALP activity was developed as blue with a

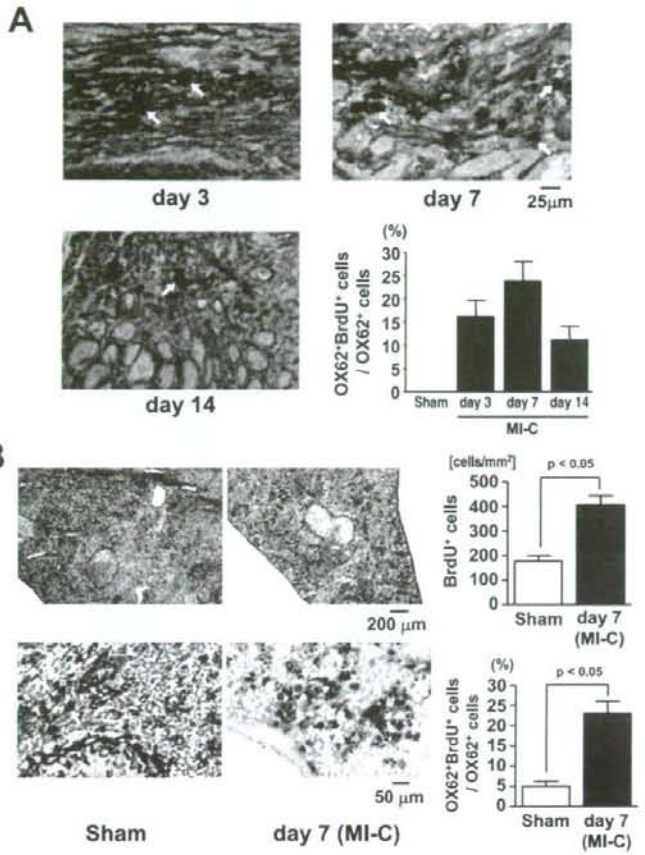


**FIGURE 3.** Proliferative response of DC after MI. Triple immunostaining of myocardium (*A*) and spleen (*B*) for OX62 (blue), BrdU (red), and type IV collagen (tissue framework; brown) was performed. Arrows indicate cells positive for both OX62 and BrdU. All figures in *A* are from border area of myocardium. Sham-operated group and MI-C group at 7 days post-MI were compared. Values are means ± SEM.

Vector blue substrate kit (Vector Laboratories). As the second step, sections were reacted with a second mAb and then with a HRP-labeled anti-mouse IgG and developed as brown with a diaminobenzidine substrate for 5–10 min. For BrdU staining, the above samples were further fixed in 1% glutaraldehyde for 10 min and digested in a pepsin solution (0.006% in 0.01 N HCl) for 10 min at 37°C. Samples were treated with 4 N HCl for 30 min at room temperature and neutralized with borate buffer (0.1 M (pH 8.5)). BrdU was detected with an anti-BrdU mAb and then with an ALP-labeled anti-mouse IgG and developed as red with a New Fuchsin substrate kit (DakoCytomation) for 5–10 min. All rats for immunohistochemical analyses received BrdU i.v. (Sigma-Aldrich; 1 mg/50 g body weight) and were sacrificed 1 h later. Slides were mounted in AquaTex (Merck) after immunostaining. Cells infiltrating the myocardium were evaluated in the infarcted, border, and noninfarcted areas.

*Immunofluorescent staining*

Immunofluorescent staining was performed for double labeling by each Ab against cell surface Ags. Mouse mAbs as described above were used as the first Abs. We applied Cy5-conjugated donkey anti-rabbit IgG (Jackson ImmunoResearch Laboratories) as the secondary Ab for type IV collagen, and a Zenon Alexa Fluor 488 mouse IgG labeling kit and Alexa Fluor 546 mouse IgG labeling kit (Invitrogen/Molecular Probes) were used as secondary reagents for mouse mAbs.

*Flow cytometric analyses*

The spleens were minced and digested in 2 mg/ml collagenase D (Roche Diagnostics) in RPMI 1640/1% FCS for 30 min at 37°C. EDTA at 10 mM was added for the last 5 min, and the cell suspension was pipetted up and down several times and filtered with a cell strainer. To lyse the RBC, ACK lysis buffer (0.15 M $NH_4Cl$, 1.0 mM $KHCO_3$, 0.1 mM $Na_2EDTA$ (pH 7.2)) was added to the cell suspension for 5 min at room temperature, and the cells were washed twice. Peripheral blood was collected into a heparinized tube. ACK lysis buffer was also added to peripheral blood for 5 min at room temperature to remove RBC. For cytometric analyses, $2 \times 10^5$ splenocytes and peripheral blood cells were incubated with PE-conjugated OX62 mAb and FITC-conjugated OX6 mAb or FITC-conjugated CD86 mAb for 40 min at 4°C. Cells were washed twice and analyzed on a Coulter EpicsXL-MCL flow cytometer (Beckman Coulter).

*Real-time quantitative RT-PCR*

After the heart had been excised, all tissues were snap frozen in liquid nitrogen and then preserved at −80°C. The LV of sham-operated rats was collected for control studies. Total RNA was isolated by a modification of the acid guanidinium thiocyanate and phenol/chloroform extraction method. After homogenizing the heart tissues with a Polytron homogenizer in TRIzol reagent (Invitrogen), total RNA was extracted with chloroform and samples were centrifuged at 16,600 × *g* for 15 min at 4°C. RNA was precipitated by addition of isopropanol, and the pellet was dissolved in diethyl pyrocarbonate water. Total RNA concentration was determined by spectrophotometric analysis at 260 nm. Reverse transcription was performed using TaqMan reagents (Applied Biosystems). Real-time quantitative PCR of each sample was conducted with TaqMan Gene Expression Assays and an ABI Prism 7700 sequence detection system (Applied Biosystems), based on methods described previously (22). The TaqMan assays used were TLR2 (Rn02133647_s1), TLR4 (Rn00569848_m1), IL-4 (Rn01456866_m1), IL-10 (Rn00563409_m1), and IFN-γ (Rn00594078_m1) from Applied Biosystems. For each sample, CT values were subtracted from that of the housekeeping gene GAPDH to generate the Ct values. Primer pairs and probe for GAPDH were as follows: forward primer, AACTCCCT

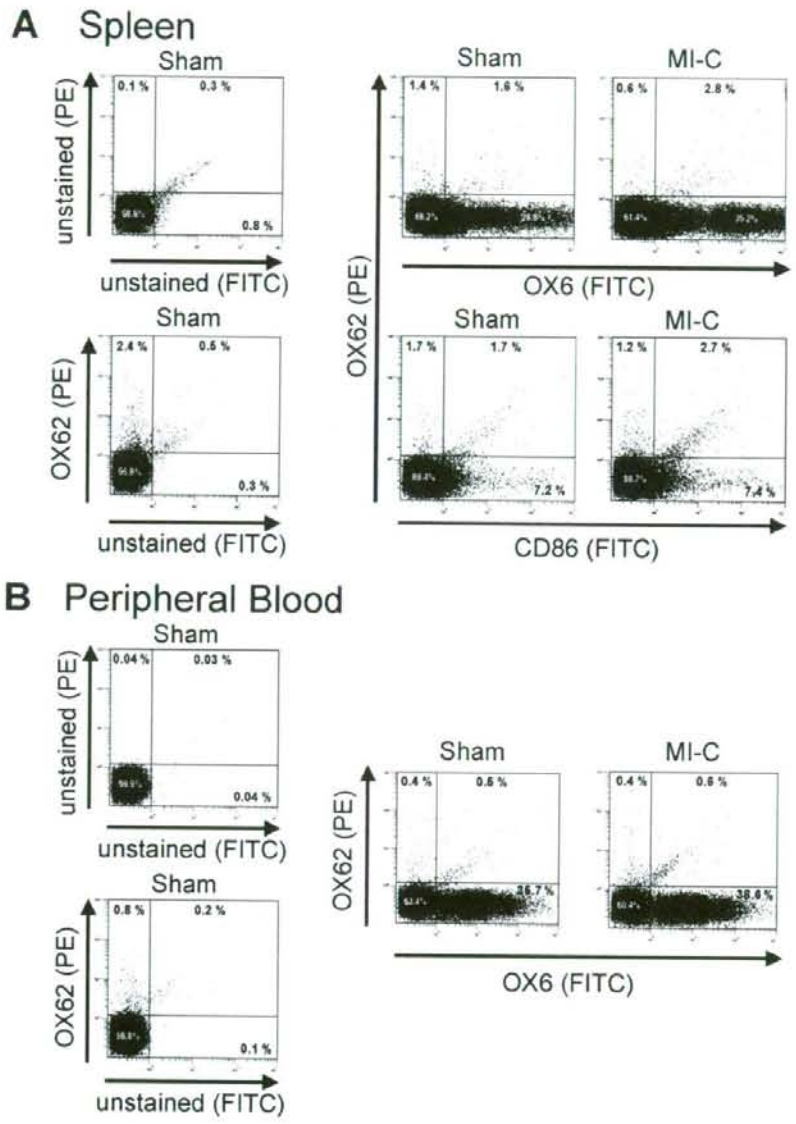


**FIGURE 4.** Respresentative flow cytometric analyses of splenocytes (*A*) and peripheral blood cells (*B*). We demonstrated analyses of unstained cells for confirmation of autofluorescent cells and cells stained with only PE-conjugated OX62 mAb from sham-operated rats in both splenocytes and peripheral blood cells. Double labeling of PE-conjugated OX62 mAb and FITC-conjugated OX6 mAb or FITC-conjugated B7-2 (CD86) mAb was performed to analyze the characteristics of OX62$^+$ cells in sham-operated group and MI-C group on day 7.

CAAGATTGTCAGCAA; reverse primer, GTGGTCATGAGCCCT TCCA; TaqMan probe: CTGCACCACCAACTGCTTAGCCCC.

*Immunoblotting analyses*

For Western blotting, frozen tissue was homogenized in cell lysis buffer (Cell Signaling Technology) containing 1% Triton X-100 and protease inhibitors. After centrifugation at 16,000 × *g* for 30 min at 4°C, the supernatant liquid was collected. Protein concentrations were measured using Coomassie protein assay reagent (Pierce Biotechnology) based on the Bradford assay. Immunoblotting analysis was conducted as previously described (22). Equal amounts of 50 μg protein were electrophoresed on 10% SDS polyacrylamide gels (150 V, 60 min). Proteins were electroblotted onto nitrocellulose membranes (Amersham Biosciences) for 60 min at 100 V. After blocking with 5% nonfat dried milk in Tris-buffered saline for 60 min, the membranes were incubated with the first Ab for 60 min, followed by exposure to the second Ab for 45 min. The immunoblots were developed by enhanced chemiluminofluorescence method. The signals were quantified by densitometry (GS-800, Bio-Rad).

*Statistical analysis*

All data were expressed as mean ± SEM. One-way ANOVA followed by Bonferroni's multiple-comparison tests was performed for statistical comparisons. All statistical analyses were performed using SPSS 13.0 for Windows. Statistical significance was defined as a $p$-value of $<0.05$.

## Results

*LV functional analyses*

Table I shows heart weight and echocardiographic and hemodynamic data on day 14. Left and right ventricular weight per body weight and LV systolic pressure in the MI-C, MI-G, and MI-GM groups did not differ significantly. Maximum dP/dt was lower and LV end-diastolic pressure (LVEDP) was higher in MI-GM than in MI-C animals. MI-GM animals had significantly larger LV end-diastolic dimension

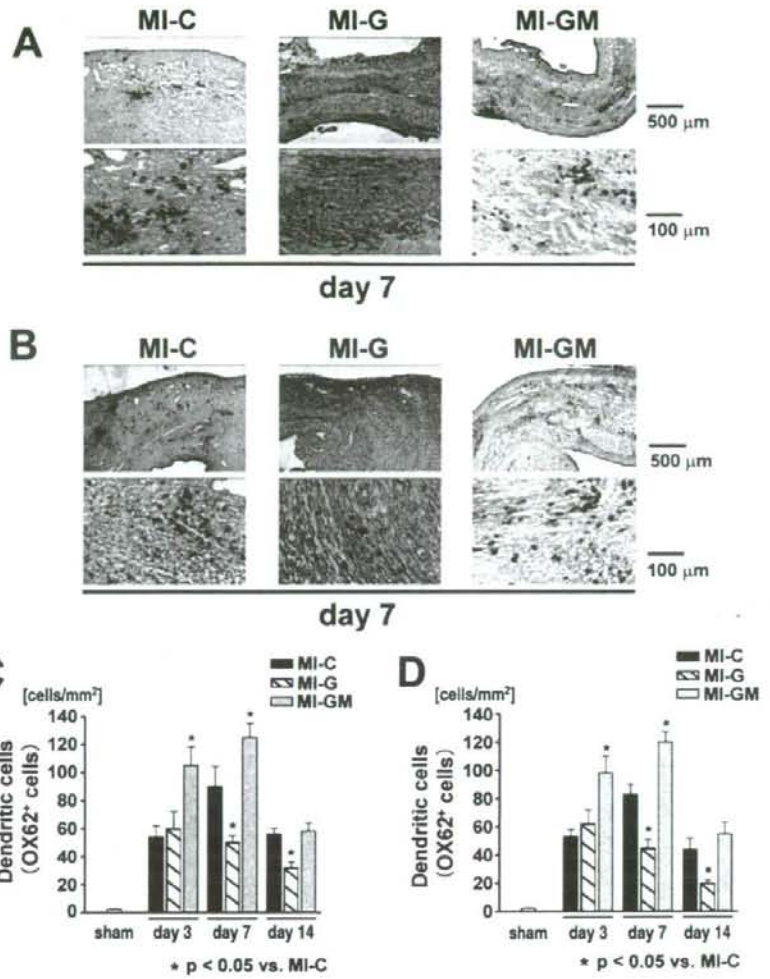


**FIGURE 5.** Effects of G-CSF and GM-CSF inducer on infiltration of DC into infarcted (*A* and *C*) and border (*B* and *D*) areas of myocardium. $OX62^+$ DC are stained blue, and type IV collagen (tissue framework) is stained brown ($n = 5$/group). All images in *A* and *B* are from day 7 after MI. Values are means ± SEM. *, $p < 0.05$ vs MI-C.

(LVEDD) and LV end-systolic dimension (LVESD), and lower fractional shortening (FS) than did MI-C animals. Higher maximum dP/dt and lower LVEDP were observed in MI-G animals than in MI-C animals. LVEDD and LVESD were smaller, and FS was greater in MI-G than in MI-C animals. Infarct size was similar in all groups.

*Infiltration of DC and MHC class II-positive cells into myocardium*

To evaluate involvement of DC in the myocardium, double immunostaining was performed with OX62, a specific marker of rat DC, and OX6 for MHC class II. Most $OX62^+$ cells were positive for OX6 (Fig. 1*A*). Serial sections were stained with V65 mAb, a marker of γδ T cells, which are known to be recognized by OX62 mAb. No $V65^+$ were detected in the myocardium of both sham-operated and MI-created rats (Fig. 1*B*). Thus, $OX62^+$ cells detected in the myocardium after MI were most probably DC. Moreover, we examined the expression of CD4 on $OX62^+$ DC that infiltrated the myocardium after MI to analyze DC subsets. Approximately 55% of $OX62^+$ cells were also $CD4^+$, and the remaining cells (45%) were $CD4^-$ (Fig. 1*C*).

The time course of DC infiltration into the infarcted, border, and noninfarcted areas in MI-C animals is shown in Fig. 1*D*. A marked increase in DC was noted in the infarcted (90 ± 9 cells/mm²) and border (83 ± 6 cells/mm²) areas, peaking on day 7. DC were rarely observed in the noninfarcted area or in the myocardium of sham-operated rats (2 ± 1 cells/mm²).

Fig. 2*A* shows the time course of MHC class II $(OX6)^+$ cell infiltration into the myocardium in MI-C group. A marked increase of MHC class $II^+$ cells was noted in all areas after MI, peaking on day 7 (infarcted area, 751 ± 39 cells/mm²; border area, 718 ± 48 cells/mm²; noninfarcted area, 105 ± 11 cells/mm²). A few MHC class $II^+$ cells were observed in the myocardium of sham-operated rats (41 ± 9 cells/mm²). Most of MHC class $II^+$ cells were $OX62^-$, $ED\text{-}1^+$ (Fig. 2*B*), and $ED\text{-}2^-$ (Fig. 2*C*), indicating a predominance of recruited infiltrating macrophages in MHC class $II^+$ cells. $ED\text{-}3^+$ cells were rarely observed in the infarcted myocardium (Fig. 2*D*). Abundant $CD45^+$ (pan-leukocyte marker) cells infiltrated the myocardium mainly from epicardial sites after MI. Infiltration of these cells was found in the infarcted heart from the early phase after MI, peaking on day 7, and was considerably decreased on day 14. $ED\text{-}1^+$ cells also infiltrated similar sites of the myocardium to $CD45^+$ cells.

*Proliferative responses of DC after MI*

Triple immunostaining for OX62, BrdU, and type IV collagen was performed to detect DC with a proliferative response

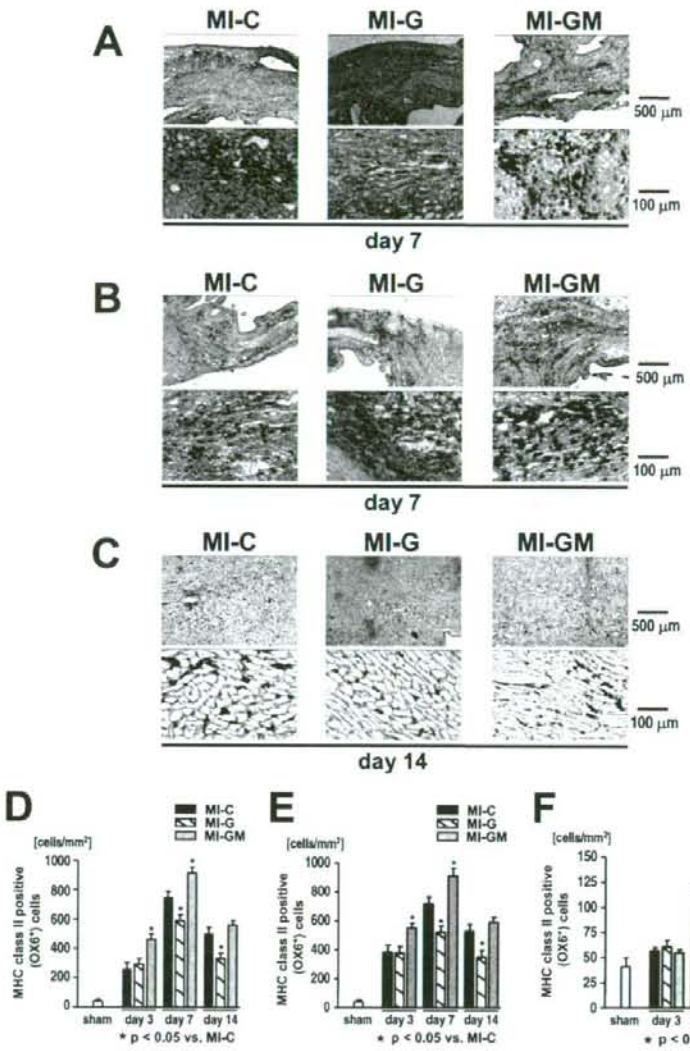


**FIGURE 6.** Effects of G-CSF and GM-CSF inducer on infiltration of MHC class II$^+$ cells into infarcted (*A* and *D*), border (*B* and *E*), and noninfarcted (*C* and *F*) myocardium. OX6$^-$ (MHC class II$^+$) cells are stained blue and type IV collagen (tissue framework) is stained brown ($n$ = 5/group). Images in *A* and *B* are from day 7, and those in *C* are from day 14 after MI. Values are means ± SEM. *, $p < 0.05$ vs MI-C.

(OX62$^+$BrdU$^+$ cells) in the myocardium after MI. OX62$^+$BrdU$^+$ cells were observed mainly in the border area on days 3, 7, and 14 (Fig. 3*A*). The ratio of OX62$^+$BrdU$^+$ cells/OX62$^+$ cells was 16% (day 3), 24% (day 7), and 11% (day14). Cells positive for OX62 or BrdU were rarely observed in the myocardium of sham-operated rats. A persistent proliferative response of DC was observed for at least 14 days after MI. These findings suggested that activated DC are present in the myocardium after MI.

To evaluate the proliferative response of DC in the spleen, we performed triple immunostaining for OX62, BrdU, and type IV collagen. The number of OX62$^+$BrdU$^+$ cells increased significantly in the spleen after MI, whereas such cells were uncommon in rats that had undergone sham operation (Fig. 3*B*). These findings indicated that MI induced activation of DC in the spleen.

*Flow cytometric analyses of splenocytes and peripheral blood cells*

OX62$^+$ cells were observed ~3% in splenocytes (Fig. 4*A*) from sham-operated rats. There was no significant difference in the number of splenic OX62$^+$ cells between sham and MI-C groups. The ratio of OX62$^+$OX6$^+$/OX62$^+$ cells in the spleen was higher in MI-C group than in sham group (Fig. 4*A*). The ratio of OX62$^+$CD86$^+$/OX62$^+$ cells was also higher in MI-C group than in sham group (Fig. 4*A*). These findings indicated that splenic DC matured after MI. There was no significant difference in the number of OX62$^+$ cells, and both OX62$^+$OX6$^+$/OX62$^+$ and OX62$^+$CD86$^+$/OX62$^+$ cell ratios in the spleen among MI-C, MI-G, and MI-GM groups. Few OX62$^+$ cells were detected in peripheral blood (Fig. 4*B*). However, there was no significant difference in the number of OX62$^+$ cells among all groups.

*Effects of G-CSF and GM-CSF inducer on infiltration of DC and MHC class II-positive cells into myocardium*

The effects of G-CSF and GM-CSF inducer on DC infiltration into the infarcted area (Fig. 5, *A* and *C*) and border area (Fig. 5, *B* and *D*) were examined. The infiltration of DC was suppressed in the MI-G group on day 7 in the infarcted (55 ± 6 vs 90 ± 9 cells/mm$^2$, $p = 0.003$) and border (51 ± 7 vs 83 ± 6 cells/mm$^2$, $p = 0.004$)

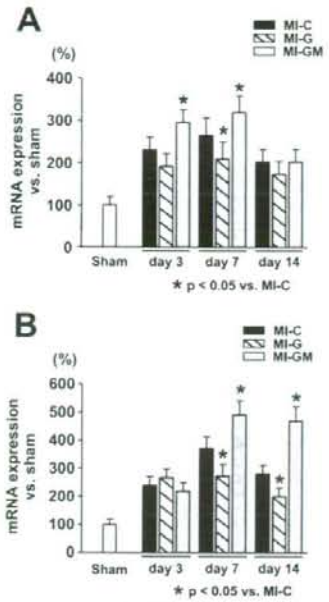


**FIGURE 7.** mRNA expression of TLR2 and TLR4 by RT-PCR. Effects of G-CSF and GM-CSF inducer on mRNA expression of TLR2 (*A*) and TLR4 (*B*). All samples except those from sham-operated rats were from infarcted area ($n$ = 5/group). Values are means ± SEM. *, $p < 0.05$ vs MI-C.

areas, and on day 14 in the infarcted (24 ± 5 vs 44 ± 5 cells/mm$^2$, $p = 0.008$) and border (20 ± 3 vs 43 ± 7 cells/mm$^2$, $p = 0.008$) areas compared with that in MI-C group (Fig. 5). The infiltration of DC was increased in the MI-GM group in the infarcted (89 ± 8 vs 54 ± 5 cells/mm$^2$, $p = 0.007$) and border (92 ± 8 vs 59 ± 7 cells/mm$^2$, $p = 0.008$) areas on day 3 and day 7 (infarcted 119 ± 5 vs 90 ± 9 cells/mm$^2$, $p = 0.011$; border 114 ± 7 vs 83 ± 6 cells/mm$^2$, $p = 0.004$) compared with the MI-C group (Fig. 5).

Fig. 6 demonstrates the effect of G-CSF and GM-CSF inducer on infiltration of MHC class II$^+$ cells into the infarcted area (Fig. 6, *A* and *D*), border area (Fig. 6, *B* and *E*), and noninfarcted area (Fig. 6, *C* and *F*) of myocardium. On day 7, positive cells were decreased in the MI-G group in the infarcted (591 ± 40 vs 751 ± 39 cells/mm$^2$, $p = 0.013$) and border (524 ± 41 vs 718 ± 48 cells/mm$^2$, $p = 0.013$) areas, and the same was found on day 14 (infarcted 332 ± 35 vs 500 ± 44 cells/mm$^2$, $p = 0.007$; border 350 ± 47 vs 531 ± 46 cells/mm$^2$, $p = 0.036$, Fig. 6, *A*, *B*, *D*, and *E*). The infiltration of MHC class II$^+$ cells was also suppressed in the noninfarcted area in the MI-G group on day 14 (61 ± 6 vs 105 ± 11 cells/mm$^2$, $p = 0.022$, Fig. 6, *C* and *F*), whereas GM-CSF inducer increased the infiltration of MHC class II$^+$ cells on day 3 in both the infarcted (460 ± 39 vs 262 ± 40 cells/mm$^2$, $p = 0.011$) and border (550 ± 33 vs 382 ± 49 cells/mm$^2$, $p = 0.016$) areas. The same was true on day 7 (infarcted area 917 ± 37 vs 751 ± 39 cells/mm$^2$, $p = 0.010$; border area 912 ± 52 vs 718 ± 48 cells/mm$^2$, $p = 0.013$, Fig. 6, *A*, *B*, *D*, and *E*). There was no significant difference in DC infiltration into the noninfarcted area between the MI-C and MI-GM groups.

*HSP70, TLR2, and TLR4 expression*

Treatment with G-CSF decreased myocardial mRNA expression of TLR2 on day 7 (Fig. 7*A*), and of TLR4 on days 7 and 14 (Fig. 7*B*) in the infarcted area compared with that in the MI-C group. In the

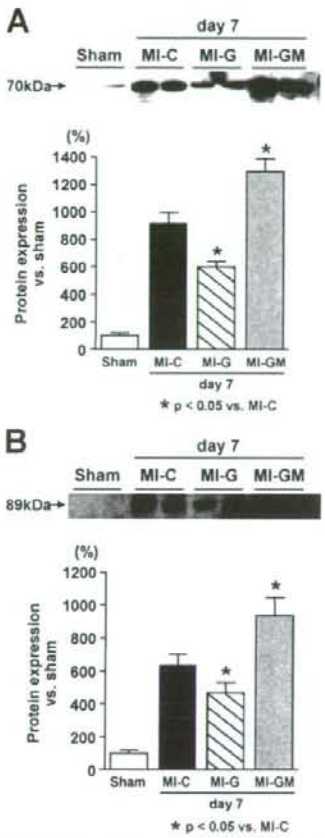


**FIGURE 8.** Immunoblotting analyses of HSP70 and TLR4 in infarcted myocardium. G-CSF suppressed and GM-CSF inducer enhanced HSP70 (*A*) and TLR4 (*B*) expression in infarcted area ($n$ = 5/group). Values are mean ± SEM. *, $p < 0.05$ vs MI-C.

MI-GM group, TLR2 expression was increased in the infarcted area on days 3 and 7 (Fig. 7*A*) and TLR4 expression was increased in the infarcted area on days 7 and 14 (Fig. 7*B*) compared with that in MI-C animals.

Immunoblotting showed that the expression of HSP70 and TLR4 proteins was significantly increased in the infarcted area, peaking on day 7 after MI, similar to the time course of DC infiltration. The expression of HSP70 and TLR4 was lower in MI-G than in MI-C animals on day 7 (Fig. 8). HSP70 and TLR4 in the infarcted area were up-regulated in MI-GM compared with those in MI-C animals (Fig. 8). Expression of HSP70 and TLR4 in the infarcted area on days 3 and 14 did not differ among the groups.

*IFN-γ and IL-10 expression in infarcted myocardium*

To evaluate the expression of both Th1 and Th2 cytokines in the infarcted myocardium after MI, we investigated the mRNA expression of IFN-γ as a representative Th1 cytokine, and of IL-4 and IL-10 as Th2 cytokines. No IL-4 was detected in this study. The expression of IFN-γ was higher in MI-GM and lower in MI-G on day 7 than in MI-C animals (Fig. 9*A*). On the other hand, the expression of IL-10 was lower in MI-GM on day 7 and higher in MI-G on days 3 and 7 than in MI-C group (Fig. 9*B*). Neither IFN-γ nor IL-10 was detected in the myocardium of sham-operated rats and MI rats on day 14.

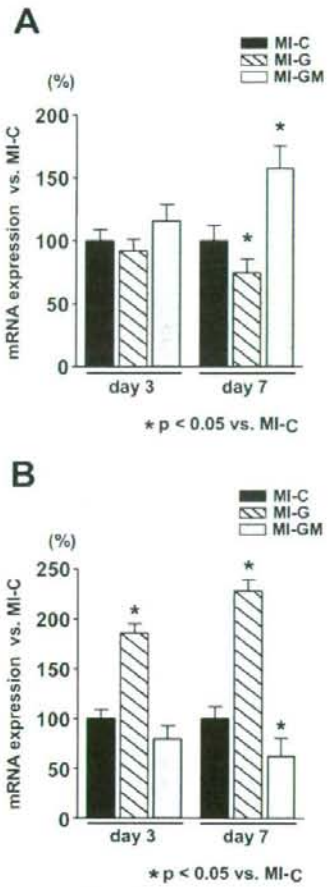


**FIGURE 9.** mRNA expression of IFN-γ (*A*) and IL-10 (*B*) on days 3 and 7 in infarcted myocardium by RT-PCR ($n$ = 5/group). Ratios of mRNA expression in MI-G and MI-GM groups are shown relative to the MI-C group. IFN-γ and IL-10 were not detected in myocardium of sham-operated rats or MI rats 14 days after surgery. Values are means ± SEM. *, $p < 0.05$ vs MI-C.

## Discussion

We demonstrated activated innate immune responses, including infiltration of $OX62^+$ DC with a proliferative response, up-regulation of HSP70 and TLRs, and increased IFN-γ and decreased IL-10 expression, in the infarcted myocardium of the rat. Our findings also revealed that MI induced proliferation and maturation of DC in the spleen. Induction of GM-CSF by romurtide increased infiltration of DC into the necrotic myocardium and adversely affected LV remodeling, whereas G-CSF administration decreased DC infiltration and improved LV function. Immunoblotting revealed that GM-CSF induction increased, but G-CSF decreased, the expression of HSP70 and TLR4 in the infarcted myocardium. Moreover, mRNA expression of TLR2, TLR4, and IFN-γ in the infarcted area was increased in MI-GM, but decreased in MI-G animals, and IL-10 was decreased in MI-GM and increased in MI-G animals. These findings suggest that CSFs regulate innate immune responses, especially DC mobilization, thereby affecting LV remodeling after MI.

Previously, Zhang et al. reported a marked increase in cells with dendrites in the infarcted and border myocardium in rat experimental MI. These investigators suggested the presence of DC by immunohistochemical staining using OX6 Ab (30). However, OX6 Ab recognizes the MHC class II molecule, which is expressed on several types of APCs as well as DC. The presence of DC in the infarcted heart has not been confirmed since their report. In the present study, using OX62, OX6, and V65 Abs and BrdU staining, we clearly demonstrated that DC infiltrate the infarcted heart in association with a proliferative response. Additionally, we confirmed that MHC class $II^+$ cells were markedly increased in the infarcted and noninfarcted myocardium after MI. Most MHC class $II^+$ cells were $OX62^-$, ED-$1^+$, and ED-$2^-$ cells, suggesting that most of these cells were recruited infiltrating macrophages (31, 32). However, it is possible that some of MHC class $II^+$ $OX62^-$ cells are also DC, because OX62 is not expressed on all DC (33). Abbate et al. described widespread myocardial inflammation in the peri-infarct and remote regions after recent MI (1). Our findings also indicated the existence of an inflammatory reaction in both infarcted and remote areas of the myocardium. Besides Ag-presenting function, cytotoxic activity has been reported in a subset of DC ($CD4^-$ subsets of $OX62^+$ DC) in the lymph nodes (34) and spleen (35). We observed both $CD4^+OX62^+$ and $CD4^-OX62^+$ DC in the infarcted myocardium. It is possible that such subsets of DC also play some role in myocardial injury after MI.

DC play critical roles in initiating and modulating immune responses and are characterized by a high capability for Ag capture and processing, migration to lymphoid organs, and expression of various costimulatory molecules. Several recent investigations revealed that endogenous toxins such as molecules released from necrotic cells can activate DC (20, 36). The heart possesses a gene-encoded innate stress response that is activated by different types of injury such as ischemia (37). Varda-Bloom et al. have shown that lymphocytes obtained from the spleen of rats that have suffered MI can injure normal cardiomyocytes (38), and Maisel et al. reported that heart failure was induced by adoptive transfer of splenic lymphocytes from rats after MI (11). Therefore, autoimmune responses against myocardial Ags may be a novel mechanism of postinfarction LV remodeling (13). Although there are few papers examining DC in the heart, a previous study using a rat permanent cerebral artery occlusion model showed that the grade of DC infiltration correlated with the extent of infarction (39). Another study using ischemia/reperfusion of rat kidney revealed infiltration and maturation of DC in infarcted renal tissue (40). Therefore, DC may play some role in secondary injury after tissue necrosis.

DC mature in lymphoid organs such as the lymph nodes and spleen after capturing Ag in peripheral tissues. Maturation of DC is essential for efficient T cell differentiation and is associated with high surface expression of MHC class II and costimulatory molecules. We observed proliferation and maturation of splenic DC after MI, indicating that MI induced intense activation of the innate immune system. The autoimmune response is regarded as one of the mechanisms of unnecessary inflammatory reactions induced secondary to myocardial injury (11–13). Our findings suggest that DC, which are potent regulators of the immune system, have a significant role in the excessive inflammatory response after MI. Moreover, the appearance of $OX62^+$ cells was not altered in peripheral blood after MI, despite dynamic movement of $OX62^+$ DC in the infarcted myocardium. These findings indicate that local expansion of DC occurred in the myocardium after MI.

Considerable evidence indicates that HSPs, especially HSP70, are potent activators of the innate immune system, which can induce production of proinflammatory cytokines by the monocyte-macrophage system and activation and maturation of DC via the TLR2 and TLR4 signal-transduction pathways (41–43). Previous reports also have shown that HSP released from necrotic cells after

tissue injury activates and matures DC through TLR stimulation (19, 20). In fact, Dybdahl et al. revealed that HSP70 is increased in the serum of MI patients and correlates with the extent of myocardial damage (44). Thus, HSP may serve as a danger signal to the innate immune system at the site of ischemic injury. Frantz et al. reported that TLR4 expression is up-regulated in failing myocardium (45) and that TLR4 plays an important role in the inflammatory response after MI (46, 47). TLR2 also is reported to contribute to ventricular remodeling (48). We found that the expression of HSP70, TLR2, and TLR4 was up-regulated after MI, peaking on day 7, similar to the time course of DC infiltration. We proposed that the increased expression of HSP70 and TLRs triggers activation of DC after MI.

DC are divided into major two subsets, myeloid and plasmacytoid. Several investigators demonstrated that GM-CSF increased myeloid DC, which induce Th1 cell differentiation, and G-CSF increased plasmacytoid DC, which induce Th2 cell differentiation (24, 25). OX62 is known to be a marker of myeloid, but not plasmacytoid, DC (33). In the present study, we revealed that G-CSF decreased and GM-CSF inducer increased the number of $OX62^+$ DC and the expression of IFN-γ in the infarcted myocardium compared with control tissue. These findings suggest that G-CSF could suppress differentiation to myeloid DC ($OX62^+$), with a decreased Th1/Th2 ratio, whereas GM-CSF facilitates differentiation to myeloid DC, with an increased Th1/Th2 ratio. A Th1/Th2 functional imbalance influences various allergic and autoimmune diseases. For example, acute coronary syndrome is associated with a Th1/Th2 balance tending to Th1 cell dominance in the myocardium (21) and peripheral blood lymphocytes (49, 50). It was reported that statins inhibited secretion of Th1 cytokines and induced secretion of Th2 cytokines (51). Statin treatment for patients with MI also resulted in decreased Th1/Th2 ratio in peripheral T cells evaluated by flow cytometry (52, 53). Moreover, Th1-polarized mice are characterized by tissue damage, which is caused by proinflammatory responses and suppression of collagen synthesis, including matrix metalloproteinase (MMP) activation and tissue inhibitor of MMP (TIMP) deactivation (54–56). In contrast, Th2 responses direct wound healing and fibrosis, which accounts for antiinflammatory responses and enhanced collagen deposition (54–56). These findings suggest that Th1/Th2 balance may disturb reparative fibrosis and facilitate infarct expansion. Therefore, the changes in DC subtypes after alteration of the Th1/Th2 balance by CSFs may influence the healing process and ventricular remodeling after MI.

This paper has several limitations. First, numerous studies have revealed that G-CSF improves ventricular remodeling and cardiac function after MI by various mechanisms in mice and rats (22, 57–59). Although previous investigators postulated that G-CSF induces regeneration, angiogenesis, and an antiapoptotic response (58–61), we did not examine such effects in the present study. Instead, we focused on its immunomodulatory effects, especially the DC-mediated innate immune response. The dose of G-CSF used was a tenth lower than that in previously described studies using a murine MI model to mobilize bone marrow stem cells into the peripheral circulation. Moreover, accumulating evidence has questioned whether G-CSF induces transdifferentiation from bone marrow progenitor cells to cardiomyocytes (62–65). Second, we could not exclude direct effects of CSFs on cardiomyocytes. Harada et al. reported G-CSF receptor expression on both adult mouse heart and cultured neonatal murine cardiomyocytes (58). The GM-CSF receptor is also reported to be expressed on human cardiomyocytes (66). Additionally, GM-CSF induction in cancer patients aggravated LV dysfunction (67). Their findings suggest that G-CSF and GM-CSF directly affect LV function. Alternatively, CSFs might affect the postinfarction healing process by modulation of other cytokines, although our previous study showed that the mRNA expression of IL-6 and TNF-α was not altered by G-CSF treatment. Third, the ratio of DC subsets in the rat spleen depends on strain (68) and OX62 is not expressed in all rat DC (33). The precise roles of all the DC subsets during LV remodeling are still undetermined. Fourth, $CD45^+$ and $CD68^+$ cells were also observed in the infarcted myocardium. We could not clarify which cell mostly operates in the healing process in this study. Further study will be required to clarify the specific role of DC during LV remodeling after MI.

In conclusion, experimental MI activates innate immunity, such as DC infiltration, HSP70 and TLR4 expression, and elevation of IFN-γ and reduction of IL-10 expression in the infarcted heart. G-CSF improves postinfarction LV remodeling in association with an attenuated innate immune reaction, whereas GM-CSF exacerbates LV remodeling with enhanced innate immunity. Suppression of DC-mediated immunity could be a new strategy to treat LV remodeling after MI.

## Acknowledgments

We thank Ms. Kyoko Ohta-Kato for technical assistance with immunostaining.

## Disclosures

The authors have no financial conflicts of interest.

## References

1. Abbate, A., E. Bonanno, A. Mauriello, R. Bussani, G. G. Biondi-Zoccai, G. Liuzzo, A. M. Leone, F. Silvestri, A. Dobrina, F. Baldi, et al. 2004. Widespread myocardial inflammation and infarct-related artery patency. *Circulation* 110: 46–50.
2. Nian, M., P. Lee, N. Khaper, and P. Liu. 2004. Inflammatory cytokines and postmyocardial infarction remodeling. *Circ. Res.* 94: 1543–1553.
3. Frangogiannis, N. G., C. W. Smith, and M. L. Entman. 2002. The inflammatory response in myocardial infarction. *Cardiovasc. Res.* 53: 31–47.
4. Anzai, T., T. Yoshikawa, H. Shiraki, Y. Asakura, M. Akaishi, H. Mitamura, and S. Ogawa. 1997. C-reactive protein as a predictor of infarct expansion and cardiac rupture after a first Q-wave acute myocardial infarction. *Circulation* 96: 778–784.
5. Takahashi, T., T. Anzai, T. Yoshikawa, Y. Maekawa, Y. Asakura, T. Satoh, H. Mitamura, and S. Ogawa. 2003. Serum C-reactive protein elevation in left ventricular remodeling after acute myocardial infarction: role of neurohormones and cytokines. *Int. J. Cardiol.* 88: 257–265.
6. Maekawa, Y., T. Anzai, T. Yoshikawa, Y. Asakura, T. Takahashi, S. Ishikawa, H. Mitamura, and S. Ogawa. 2002. Prognostic significance of peripheral monocytosis after reperfused acute myocardial infarction: a possible role for left ventricular remodeling. *J. Am. Coll. Cardiol.* 39: 241–246.
7. Roberts, R., V. DeMello, and B. E. Sobel. 1976. Deleterious effects of methylprednisolone in patients with myocardial infarction. *Circulation* 53 (Suppl. 3): 1204–1206.
8. Hammerman, H., R. A. Kloner, F. Hale, F. J. Schoen, and E. Braunwald. 1983. Dose-dependent effects of short-term methylprednisolone on myocardial infarct extent, scar formation and ventricular function. *Circulation* 68: 446–453.
9. Brown, E. J., Jr., R. A. Kloner, F. J. Schoen, H. Hammerman, S. Hale, and E. Braunwald. 1983. Scar thinning due to ibuprofen administration after experimental myocardial infarction. *Am. J. Cardiol.* 51: 877–883.
10. Jugdutt, B. I. 1985. Delayed effects of early infarct-limiting therapies on healing after myocardial infarction. *Circulation* 72: 907–914.
11. Maisel, A., D. Cesario, S. Baird, J. Rehman, P. Haghighi, and S. Carter. 1998. Experimental autoimmune myocarditis produced by adoptive transfer of splenocytes after myocardial infarction. *Circ. Res.* 82: 458–463.
12. Moraru, M., A. Roth, G. Keren, and J. George. 2006. Cellular autoimmunity to cardiac myosin in patients with a recent myocardial infarction. *Int. J. Cardiol.* 107: 61–66.
13. Liao, Y. H., and X. Cheng. 2006. Autoimmunity in myocardial infarction. *Int. J. Cardiol.* 112: 21–26.
14. De Scheerder, I., J. Vandekerckhove, J. Robbrecht, L. Algoed, M. De Buyzere, J. De Langhe, G. De Schrijver, and D. Clement. 1985. Post-cardiac injury syndrome and an increased humoral immune response against the major contractile proteins (actin and myosin). *Am. J. Cardiol.* 56: 631–633.
15. Eriksson, S., J. Hellman, and K. Pettersson. 2005. Autoantibodies against cardiac troponins. *N. Engl. J. Med.* 352: 98–100.
16. Banchereau, J., and R. M. Steinman. 1998. Dendritic cells and the control of immunity. *Nature* 392: 245–252.
17. Mellman, I., and R. M. Steinman. 2001. Dendritic cells: specialized and regulated antigen processing machines. *Cell* 106: 255–258.
18. Steinman, R. M. 1991. The dendritic cell system and its role in immunogenicity. *Annu. Rev. Immunol.* 9: 271–296.

19. Millar, D. G., K. M. Garza, B. Odermatt, A. R. Elford, N. Ono, Z. Li, and P. S. Ohashi. 2003. Hsp70 promotes antigen-presenting cell function and converts T-cell tolerance to autoimmunity in vivo. *Nat. Med.* 9: 1469–1476.
20. Sauter, B., M. L. Albert, L. Francisco, M. Larsson, S. Somersan, and N. Bhardwaj. 2000. Consequences of cell death: exposure to necrotic tumor cells, but not primary tissue cells or apoptotic cells, induces the maturation of immunostimulatory dendritic cells. *J. Exp. Med.* 191: 423–434.
21. Cheng, X., Y. H. Liao, H. Ge, B. Li, J. Zhang, J. Yuan, M. Wang, Y. Liu, Z. Guo, J. Chen, et al. 2005. TH1/TH2 functional imbalance after acute myocardial infarction: coronary arterial inflammation or myocardial inflammation. *J. Clin. Immunol.* 25: 246–253.
22. Sugano, Y., T. Anzai, T. Yoshikawa, Y. Maekawa, T. Kohno, K. Mahara, K. Naito, and S. Ogawa. 2005. Granulocyte colony-stimulating factor attenuates early ventricular expansion after experimental myocardial infarction. *Cardiovasc. Res.* 65: 446–456.
23. Maekawa, Y., T. Anzai, T. Yoshikawa, Y. Sugano, K. Mahara, T. Kohno, T. Takahashi, and S. Ogawa. 2004. Effect of granulocyte-macrophage colony-stimulating factor inducer on left ventricular remodeling after acute myocardial infarction. *J. Am. Coll. Cardiol.* 44: 1510–1520.
24. Bottomly, K. 1999. T cells and dendritic cells get intimate. *Science* 283: 1124–1125.
25. Arpinati, M., C. L. Green, S. Heimfeld, J. E. Heuser, and C. Anasetti. 2000. Granulocyte-colony stimulating factor mobilizes T helper 2-inducing dendritic cells. *Blood* 95: 2484–2490.
26. Shaughnessy, P. J., C. Bachier, C. F. Lemaistre, C. Akay, B. H. Pollock, and Y. Gazitt. 2006. Granulocyte colony-stimulating factor mobilizes more dendritic cell subsets than granulocyte-macrophage colony-stimulating factor with no polarization of dendritic cell subsets in normal donors. *Stem Cells* 24: 1789–1797.
27. Brenan, M., and M. Puklavec. 1992. The MRC OX-62 antigen: a useful marker in the purification of rat veiled cells with the biochemical properties of an integrin. *J. Exp. Med.* 175: 1457–1465.
28. Saiki, T., T. Ezaki, M. Ogawa, and K. Matsuno. 2001. Trafficking of host- and donor-derived dendritic cells in rat cardiac transplantation: allosensitization in the spleen and hepatic nodes. *Transplantation* 71: 1806–1815.
29. Matsuno, K., T. Ezaki, S. Kudo, and Y. Uehara. 1996. A life stage of particle-laden rat dendritic cells in vivo: their terminal division, active phagocytosis, and translocation from the liver to the draining lymph. *J. Exp. Med.* 183: 1865–1878.
30. Zhang, J., Z. X. Yu, S. Fujita, M. L. Yamaguchi, and V. J. Ferrans. 1993. Interstitial dendritic cells of the rat heart: quantitative and ultrastructural changes in experimental myocardial infarction. *Circulation* 87: 909–920.
31. Damoiseaux, J. G., E. A. Dopp, W. Calame, D. Chao, G. G. MacPherson, and C. D. Dijkstra. 1994. Rat macrophage lysosomal membrane antigen recognized by monoclonal antibody ED1. *Immunology* 83: 140–147.
32. Honda, H., H. Kimura, and A. Rostami. 1990. Demonstration and phenotypic characterization of resident macrophages in rat skeletal muscle. *Immunology* 70: 272–277.
33. Hubert, F. X., C. Voisine, C. Louvet, M. Heslan, and R. Josien. 2004. Rat plasmacytoid dendritic cells are an abundant subset of MHC class II$^+$ CD4$^+$ CD11b$^-$OX62$^-$ and type I IFN-producing cells that exhibit selective expression of Toll-like receptors 7 and 9 and strong responsiveness to CpG. *J. Immunol.* 172: 7485–7494.
34. Liu, L., M. Zhang, C. Jenkins, and G. G. MacPherson. 1998. Dendritic cell heterogeneity in vivo: two functionally different dendritic cell populations in rat intestinal lymph can be distinguished by CD4 expression. *J. Immunol.* 161: 1146–1155.
35. Trinite, B., C. Voisine, H. Yagita, and R. Josien. 2000. A subset of cytolytic dendritic cells in rat. *J. Immunol.* 165: 4202–4208.
36. Gallucci, S., M. Lolkema, and P. Matzinger. 1999. Natural adjuvants: endogenous activators of dendritic cells. *Nat. Med.* 5: 1249–1255.
37. Knuefermann, P., J. Vallejo, and D. L. Mann. 2004. The role of innate immune responses in the heart in health and disease. *Trends Cardiovasc. Med.* 14: 1–7.
38. Varda-Bloom, N., J. Leor, D. G. Ohad, Y. Hasin, M. Amar, R. Fixler, A. Battler, M. Eldar, and D. Hasin. 2000. Cytotoxic T lymphocytes are activated following myocardial infarction and can recognize and kill healthy myocytes in vitro. *J. Mol. Cell. Cardiol.* 32: 2141–2149.
39. Kostulas, N., H. L. Li, B. G. Xiao, Y. M. Huang, V. Kostulas, and H. Link. 2002. Dendritic cells are present in ischemic brain after permanent middle cerebral artery occlusion in the rat. *Stroke* 33: 1129–1134.
40. Kim, B. S., S. W. Lim, C. Li, J. S. Kim, B. K. Sun, K. O. Ahn, S. W. Han, J. Kim, and C. W. Yang. 2005. Ischemia-reperfusion injury activates innate immunity in rat kidneys. *Transplantation* 79: 1370–1377.
41. Asea, A., S. K. Kraeft, E. A. Kurt-Jones, M. A. Stevenson, L. B. Chen, R. W. Finberg, G. C. Koo, and S. K. Calderwood. 2000. HSP70 stimulates cytokine production through a CD14-dependant pathway, demonstrating its dual role as a chaperone and cytokine. *Nat. Med.* 6: 435–442.
42. Vabulas, R. M., P. Ahmad-Nejad, S. Ghose, C. J. Kirschning, R. D. Issels, and H. Wagner. 2002. HSP70 as endogenous stimulus of the Toll/interleukin-1 receptor signal pathway. *J. Biol. Chem.* 277: 15107–15112.
43. Wallin, R. P., A. Lundqvist, S. H. More, A. von Bonin, R. Kiessling, and H. G. Ljunggren. 2002. Heat-shock proteins as activators of the innate immune system. *Trends Immunol.* 23: 130–135.
44. Dybdahl, B., S. A. Slordahl, A. Waage, P. Kierulf, T. Espevik, and A. Sundan. 2005. Myocardial ischaemia and the inflammatory response: release of heat shock protein 70 after myocardial infarction. *Heart* 91: 299–304.
45. Frantz, S., L. Kobzik, Y. D. Kim, R. Fukazawa, R. Medzhitov, R. T. Lee, and R. A. Kelly. 1999. Toll4 (TLR4) expression in cardiac myocytes in normal and failing myocardium. *J. Clin. Invest.* 104: 271–280.
46. Oyama, J., C. Blais, Jr., X. Liu, M. Pu, L. Kobzik, R. A. Kelly, and T. Bourcier. 2004. Reduced myocardial ischemia-reperfusion injury in Toll-like receptor 4-deficient mice. *Circulation* 109: 784–789.
47. Dybdahl, B., A. Wahba, E. Lien, T. H. Flo, A. Waage, N. Qureshi, O. F. Sellevold, T. Espevik, and A. Sundan. 2002. Inflammatory response after open heart surgery: release of heat-shock protein 70 and signaling through Toll-like receptor-4. *Circulation* 105: 685–690.
48. Shishido, T., N. Nozaki, S. Yamaguchi, Y. Shibata, J. Nitobe, T. Miyamoto, H. Takahashi, T. Arimoto, K. Maeda, M. Yamakawa, et al. 2003. Toll-like receptor-2 modulates ventricular remodeling after myocardial infarction. *Circulation* 108: 2905–2910.
49. Methe, H., S. Brunner, D. Wiegand, M. Nabauer, J. Koglin, and E. R. Edelman. 2005. Enhanced T-helper-1 lymphocyte activation patterns in acute coronary syndromes. *J. Am. Coll. Cardiol.* 45: 1939–1945.
50. Soejima, H., A. Irie, S. Miyamoto, I. Kajiwara, S. Kojima, J. Hokamaki, T. Sakamoto, T. Tanaka, M. Yoshimura, Y. Nishimura, and H. Ogawa. 2003. Preference toward a T-helper type 1 response in patients with coronary spastic angina. *Circulation* 107: 2196–2200.
51. Youssef, S., O. Stuve, J. C. Patarroyo, P. J. Ruiz, J. L. Radosevich, E. M. Hur, M. Bravo, D. J. Mitchell, R. A. Sobel, L. Steinman, and S. S. Zamvil. 2002. The HMG-CoA reductase inhibitor, atorvastatin, promotes a Th2 bias and reverses paralysis in central nervous system autoimmune disease. *Nature* 420: 78–84.
52. Cheng, X., Y. H. Liao, J. Zhang, B. Li, H. Ge, J. Yuan, M. Wang, B. Lu, Y. Liu, and Y. Cheng. 2005. Effects of atorvastatin on Th polarization in patients with acute myocardial infarction. *Eur. J. Heart Fail.* 7: 1099–1104.
53. Shimada, K., K. Miyauchi, and H. Daida. 2004. Early intervention with atorvastatin modulates TH1/TH2 imbalance in patients with acute coronary syndrome: from bedside to bench. *Circulation* 109: e213–e214.
54. Wynn, T. A. 2004. Fibrotic disease and the $T_H1/T_H2$ paradigm. *Nat. Rev. Immunol.* 4: 583–594.
55. Shi, Z., A. E. Wakil, and D. C. Rockey. 1997. Strain-specific differences in mouse hepatic wound healing are mediated by divergent T helper cytokine responses. *Proc. Natl. Acad. Sci. USA* 94: 10663–10668.
56. Sandler, N. G., M. M. Mentink-Kane, A. W. Cheever, and T. A. Wynn. 2003. Global gene expression profiles during acute pathogen-induced pulmonary inflammation reveal divergent roles for Th1 and Th2 responses in tissue repair. *J. Immunol.* 171: 3655–3667.
57. Minatoguchi, S., G. Takemura, X. H. Chen, N. Wang, Y. Uno, M. Koda, M. Arai, Y. Misao, C. Lu, K. Suzuki, et al. 2004. Acceleration of the healing process and myocardial regeneration may be important as a mechanism of improvement of cardiac function and remodeling by postinfarction granulocyte colony-stimulating factor treatment. *Circulation* 109: 2572–2580.
58. Harada, M., Y. Qin, H. Takano, T. Minamino, Y. Zou, H. Toko, M. Ohtsuka, K. Matsuura, M. Sano, J. Nishi, et al. 2005. G-CSF prevents cardiac remodeling after myocardial infarction by activating the Jak-Stat pathway in cardiomyocytes. *Nat. Med.* 11: 305–311.
59. Jackson, K. A., S. M. Majka, H. Wang, J. Pocius, C. J. Hartley, M. W. Majesky, M. L. Entman, L. H. Michael, K. K. Hirschi, and M. A. Goodell. 2001. Regeneration of ischemic cardiac muscle and vascular endothelium by adult stem cells. *J. Clin. Invest.* 107: 1395–1402.
60. Orlic, D., J. Kajstura, S. Chimenti, I. Jakoniuk, S. M. Anderson, B. Li, J. Pickel, R. McKay, B. Nadal-Ginard, D. M. Bodine, et al. 2001. Bone marrow cells regenerate infarcted myocardium. *Nature* 410: 701–705.
61. Kocher, A. A., M. D. Schuster, M. J. Szabolcs, S. Takuma, D. Burkhoff, J. Wang, S. Homma, N. M. Edwards, and S. Itescu. 2001. Neovascularization of ischemic myocardium by human bone-marrow-derived angioblasts prevents cardiomyocyte apoptosis, reduces remodeling and improves cardiac function. *Nat. Med.* 7: 430–436.
62. Balsam, L. B., A. J. Wagers, J. L. Christensen, T. Kofidis, I. L. Weissman, and R. C. Robbins. 2004. Haematopoietic stem cells adopt mature haematopoietic fates in ischaemic myocardium. *Nature* 428: 668–673.
63. Murry, C. E., M. H. Soonpaa, H. Reinecke, H. Nakajima, H. O. Nakajima, M. Rubart, K. B. Pasumarthi, J. I. Virag, S. H. Bartelmez, V. Poppa, et al. 2004. Haematopoietic stem cells do not transdifferentiate into cardiac myocytes in myocardial infarcts. *Nature* 428: 664–668.
64. Wagers, A. J., R. I. Sherwood, J. L. Christensen, and I. L. Weissman. 2002. Little evidence for developmental plasticity of adult hematopoietic stem cells. *Science* 297: 2256–2259.
65. Taylor, D. A., R. Hruban, E. R. Rodriguez, and P. J. Goldschmidt-Clermont. 2002. Cardiac chimerism as a mechanism for self-repair: does it happen and if so to what degree? *Circulation* 106: 2–4.
66. Postiglione, L., S. Montagnani, P. Ladogana, C. Castaldo, G. Di Spigna, E. M. Bruno, M. Turano, L. De Santo, G. Cudemo, S. Cocozza, et al. 2006. Granulocyte macrophage-colony stimulating factor receptor expression on human cardiomyocytes from end-stage heart failure patients. *Eur. J. Heart Fail.* 8: 564–570.
67. Knoops, S., A. B. Groeneveld, O. Kamp, W. K. Lagrand, and K. Hoekman. 2001. Granulocyte-macrophage colony-stimulating factor (GM-CSF) decreases left ventricular function: an echocardiographic study in cancer patients. *Cytokine* 14: 184–187.
68. Hubert, F. X., C. Voisine, C. Louvet, J. M. Heslan, A. Ouabed, M. Heslan, and R. Josien. 2006. Differential pattern recognition receptor expression but stereotyped responsiveness in rat spleen dendritic cell subsets. *J. Immunol.* 177: 1007–1016.

Journal of the American College of Cardiology
© 2008 by the American College of Cardiology Foundation
Published by Elsevier Inc.

Vol. 51, No. 20, 2008
ISSN 0735-1097/08/$34.00
doi:10.1016/j.jacc.2008.01.050

**PRECLINICAL RESEARCH**

# Clarithromycin Attenuates Acute and Chronic Rejection Via Matrix Metalloproteinase Suppression in Murine Cardiac Transplantation

Masahito Ogawa, BS,* Jun-ichi Suzuki, MD,* Keiichi Hishikari, BS,* Kiyoshi Takayama, PHD,* Hiroyuki Tanaka, MD, PHD,† Mitsuaki Isobe, MD, PHD*

*Tokyo, Japan*

**Objectives** Clarithromycin (CAM), a major macrolide antibiotic, has many biological functions, including matrix metalloproteinases (MMPs) regulation. However, little is known about the effect of CAM in heart transplantation via MMP-9. The purpose of this study was to clarify the role of MMPs regulated by CAM in the progression of rejection.

**Background** The MMPs are critical in the development of inflammation and tissue remodeling. The MMP-9 level is associated with the rejection of heart transplantation.

**Methods** We orally administered CAM into murine cardiac allograft recipients. Total allomismatch combination and class II mismatch combination were used for the analysis of graft survival, pathology and molecular.

**Results** Clarithromycin improved acute rejection judged by graft survival and by myocardial cell infiltrating area in a total allomismatch combination. The CAM-treated allografts showed affected expression of T-cells, macrophages, and MMP-9 in immunohistochemistry. Zymography indicated that enhanced MMPs activities were observed in nontreated hearts, whereas CAM suppressed the levels. In chronic rejection, CAM suppressed the development of graft arterial disease and myocardial remodeling compared with that of nontreatment. Clarithromycin inhibited the expression of MMP-9, whereas the treatment did not alter the expression of MMP-2 and tissue inhibitor metalloproteinase-1 in macrophages and smooth muscle cells. Inhibition of MMP-9 by CAM was associated with suppression of smooth muscle cell migration and proliferation.

**Conclusions** Clarithromycin is useful to suppress allograft remodeling, because it is critically involved in the prevention of cardiac rejection through the suppression of MMP-9. (J Am Coll Cardiol 2008;51:1977–85) © 2008 by the American College of Cardiology Foundation

Acute cardiac rejection is still a major complication of heart transplantation. Inflammatory factors such as cytokines, chemokines, and adhesion molecules play a critical role in the development of acute rejection (1–3). The allografts show diffuse arterial neointimal formation (graft arterial disease [GAD]), that consists of smooth muscle cells (SMCs), extracellular matrix (ECM), and variously mononuclear leukocytes during long-term observation. Although GAD ultimately culminates in vascular stenosis and ischemic graft failure, the infallible care and prevention measures are still unknown.

Clarithromycin (CAM) is known as a 14-member ring macrolide and a potent antibiotic for the treatment of various microbial infections. Recently, CAM has been reported to have multiple biologic effects, such as alteration of inflammatory factors (4,5). Many inflammatory cells, such as lymphocytes (6,7) and monocytes/macrophages (8,9), produce matrix metalloproteinases (MMPs), and levels have been shown to be upregulated in grafts with human and various mammal organ transplantation (10–12). The MMPs are a large family of proteinases that proteolytically degrade ECM such as collagen and proteoglycan. The degradation of ECM is an important event in the process of inflammation and tissue remodeling. A member of MMPs, MMP-9 (gelatinase B) is known to play an important role in tissue remodeling and the migration of various cells, such as SMCs (13,14), macrophages, and other cells. Smooth muscle cells are shown to express MMP-2 and -9, and excess activation of MMP-2 and -9 induce the destruction of the ECM and can lead to

From the Departments of *Cardiovascular Medicine and †Thoracic Surgery, Tokyo Medical and Dental University, Tokyo, Japan. This work was supported by grants from the Japan Cardiovascular Research Foundation, a Grant-in-aid from the Japanese Ministry of Education, Science and Culture, a Grant-in-aid from the Japanese Ministry of Welfare, and the Organization for Pharmaceutical Safety and Research.

Manuscript received October 17, 2007; revised manuscript received December 13, 2007, accepted January 21, 2008.

JACC Vol. 51, No. 20, 2008
May 20, 2008:1977–85

**Abbreviations and Acronyms**

CAM = clarithromycin
GAD = graft arterial disease
DMEM = Dulbecco's modified Eagle's medium
ICAM = intercellular adhesion molecule
IL = interleukin
MHC = major histocompatibility complex
MMP = matrix metalloproteinase
mRNA = messenger ribonucleic acid
NF-κB = nuclear factor-kappa B
RNA = ribonucleic acid
SMC = smooth muscle cell
TIMP = tissue inhibitor metalloproteinase

pathological remodeling and vascular restenosis. However, little is known about the role of MMP-9 for acute and chronic rejection in heart transplantation. This study demonstrated that CAM suppressed acute and chronic rejection through the inhibition of the MMP-9 expression from mononuclear cells and SMCs.

## Methods

**Reagents.** The CAM was kindly provided by Taisho Toyama Pharmaceutical Corporation, Ltd (Tokyo, Japan).

**Experimental animals and cardiac transplantation.** The male BALB/c (H-$2^d$) and C57BL/6 (H-$2^b$) mice (4 to 6 weeks, 20 to 25 g) were obtained from Japan Clea Corporation (Tokyo, Japan), and this combination was used as the major histocompatibility complex (MHC) total allomismatch group for analysis of acute rejection (8 animals for graft survival analysis in each group). A combination of male C57BL/6 Bm12 (H-$2^{bm12}$) and C57BL/6 mice (4 to 6 weeks, 20 to 25 g) was used as the MHC class II mismatch group for analysis of chronic rejection (n = 6 each group). Heterotopic cardiac transplantation was performed as described previously (15). Recipient mice were given oral administration CAM (100 mg/kg/day) twice/day. We selected the dose for mice on the basis of previous papers (16,17). Graft survival and function were evaluated by daily palpation, and cessation of beating was interpreted as rejection as previously reported (18). The mortality rate induced by surgical or technical failure of this murine heart transplant procedure is <2% in our laboratory. This investigation conforms with the Guide for the Care and Use of Laboratory Animals in the Tokyo Medical and Dental University.

**Histopathology.** Histopathological analysis was performed as described previously (19). We obtained 5 transverse sections/heart for histopathologic examination. The sections were stained with hematoxylin and eosin, Elastica van Gieson, and Mallory. The area of myocardium and surrounding tissue affected by acute rejection and chronic rejection were determined with a computer-assisted analyzer (Image-Pro Express, Nikon, Tokyo, Japan). The area ratio (affected/entire area as a percentage) was calculated as described previously (15). All data were analyzed in a blind fashion by 2 independent investigators and averaged. Samples from 9 animals in each group of the total allomismatch combination and 6 animals in each group of the MHC class II mismatch combination were used for histological analysis.

**Film in situ zymography.** Film in situ zymography was performed as described previously (20). Frozen sections were cut to a thickness of 7 μm (4 samples in each group). These sections were mounted on polyethylenetelephthalate film coated with gelatin (FIZ-GN) (Wako Pure Chemical Industries, Ltd., Osaka, Japan). As a control, these sections were mounted on polyethylenetelephthalate film coated with gelatin and an MMP inhibitor (FIZ-GI) (Wako). Frozen sections on these films were incubated in a moist chamber at 37°C for 6 h. After incubation, these films dried for 30 min and were then stained with Biebrich Scarlet Stain Solution (Wako) for 4 min. Gelatinolytic activity is visible as a clear area unstained by Biebrich Scarlet; this solution stains only gelatin on the film, leaving areas with gelatinolytic activity unstained and bright.

**Immunohistochemistry.** Sections (4 samples in each group) were incubated with primary antibodies against murine intercellular adhesion molecule (ICAM)-1 (YN1/1.7) (provided by Professor Ko Okumura, Juntendo University), CD4, CD8, CA11b (BD Biosciences Pharmingen, San Diego, California), nuclear factor-kappa B (NF-κB) p65, or MMP-9 (Santa Cruz Biotechnology, Inc., Santa Cruz, California) at 4°C for 12 h. Antibody-HRP conjugate was detected with Histofine Simplestain Kit (Nichirei Corporation, Tokyo, Japan), used according to the manufacturer's instructions. Enzyme activity was detected with 3-Amino-9-ethylcarbazole.

**Ribonuclease protection assay.** Trizol (Invitrogen Corporation, Carlsbad, California) was used to isolate total ribonucleic acid (RNA) according to the manufacturer's protocol. The probe was synthesized by the in vitro transcription method with a Multi-Probe Template Set mCK-1 (Pharmingen), T7 polymerase, and [$^{32}$P] UTP. Messenger ribonucleic acid (mRNA) levels were quantified and normalized against levels of glyceraldehyde-3-phosphate dehydrogenases (GAPDH) (4 samples in each group).

**Cell preparations.** Primary SMCs were obtained from the thoracic aortas of Bm12 mice by the explant technique described previously (19). The SMCs were grown with Dulbecco's modified Eagle's medium (DMEM) (Sigma Chemical Corporation, St. Louis, Missouri) supplemented 50 μg/ml streptomycin, 50 IU/ml penicillin, and 10% fetal bovine serum at 37°C and 5% carbon dioxide. The J774.1A (BALB/cA) cells were obtained from Riken Bioresource Center (Tsukuba, Japan) and were grown with RPMI1640 (Sigma) supplemented 10% fetal bovine serum.

**Western blotting.** Western blot analysis was described previously (21). The polyvinylidene difluoride membrane incubated with primary antibody MMP-9, MMP-2, and beta-actin (Santa Cruz). And then, the membrane enhanced chemiluminescence reagent (Pierce Biotechnology Inc., Rockford, Illinois). Enhanced chemiluminescence was detected with an LAS-1000 (Fujifilm Corporation, Tokyo, Japan). The data were obtained from 3 independent experiments (4 samples in each group).

**Table 1** Using RT-PCR Primer Design for Mice

| Name | Sequences | Molecular Weight | GenBank |
|---|---|---|---|
| MMP-9 | Forward 5'-TGT TCA GCA AGG GGC GTG TC-3'<br>Reverse 5'-AAA CAG TCC AAC AAG AAA GG-3' | 461 bp | NM_013599 |
| MMP-2 | Forward 5'-GGC CAT GCC ATG GGG CTG GA-3'<br>Reverse 5'-CCA GTC TGA TTT GAT GCT TC-3' | 762 bp | NM_008610 |
| TIMP-1 | Forward 5'-CTG GCA TCC TCT TGT TGC TA-3'<br>Reverse 5'-AGG GAT CTC CAG GTG CAC AA-3' | 585 bp | NM_011593 |
| GAPDH | Forward 5'-TGA AGG TCG GTG TGA ACG GAT TTG GC-3'<br>Reverse 5'-CAT GTA GGC CAT GAG GTC CAC CAC-3' | 983 bp | NM_001001303 |

bp = base pair; GAPDH = glyceraldehyde-3-phosphate dehydrogenases; MMP = matrix metalloproteinase; RT-PCR = reverse transcriptase-polymerase chain reaction; TIMP = tissue inhibitor metalloproteinase.

**Reverse transcriptase-polymerase chain reaction.** Serum-starved-J774.1A cells were stimulated with interleukin (IL)-1beta recombinant (10 ng/ml) (R&D Systems, Minneapolis, Minnesota). Serum-starved SMCs were stimulated with PDGF-BB (5 ng/ml) (Biosource International, Camarillo, California). Total RNA were collected 16 h after stimulation and isolated according to the manufacture's protocol by Trizol (Invitrogen). Complementary deoxyribonucleic acid was prepared with the reverse transcriptase-polymerase chain reaction (RT-PCR) kit. The PCR was performed with PCR-kit in the presence of oligo-primers for MMP-9, MMP-2, tissue inhibitor metalloproteinase (TIMP)-1, and GAPDH. The data were obtained from 3 independent experiments (4 samples in each group) (Table 1).

**Transmigration assay.** The migration assay was performed as described previously (9,22). Briefly, the assay was performed with Transwell chambers (Corning Corporation, Corning, New York) 24-well tissue culture plates composed of 5 $\mu$m pore polycarbonate filters. The upper chambers were not coated. The SMCs were seeded at $1 \times 10^4$ cells/well in 100 $\mu$l medium. The lower chamber was filled with 400 $\mu$l of DMEM medium supplemented with 5 ng/ml PDGF-BB and 0.5% fetal bovine serum (FBS), and then the chambers were incubated at 37°C for 24 h in 5% carbon dioxide incubator. Cells were counted under a microscope, and the cells that migrated to the lower chamber were examined. The data were obtained from 3 independent experiments (4 samples in each group).

**Proliferation assay.** The SMCs were seeded on the 96-well plates ($5 \times 10^3$ cells/well) and then incubated with DMEM supplemented 0.5% FBS and PDGF-BB for 2 days in incubator. Cell proliferation was then assessed with the Cell Counting Kit-8 (Dojindo, Kumamoto, Japan) according to the manufacturer's instructions. Cell proliferation was expressed as the optical density (15). The data were obtained from 3 independent experiments (6 samples in each group).

**Statistical analysis.** All data are expressed as mean ± SEM. Kaplan-Meier analysis was used to estimate graft survival, and the Mann-Whitney *U* test was used for survival differences between the 2 groups. Data were compared, and differences between the 2 groups were analyzed by the Student *t* test for histopathological analysis and ribonuclease protection assay. One-way analysis of variance was used in the SMC proliferation assay and SMC migration assay. Differences with values of $p < 0.05$ were considered significant.

## Results

**Graft survival prolonged and affected the histopathology by CAM.** In the major mismatch group, nontreated allografts were acutely rejected (7.3 ± 0.2 days, n = 8). However, CAM administration significantly prolonged allograft survival (9.7 ± 0.2 days, $p < 0.05$, n = 8) in this model (Fig. 1). Moderate myocardial cell infiltration was observed in nontreated allografts on day 7 (35.7 ± 1.9%, n = 9), whereas CAM treatment markedly attenuated myocardial cell infiltration (19.7 ± 3.0%, $p < 0.05$, n = 9) (Figs. 2A and 2B). Although significant fibrosis was observed in the nontreated allografts (39.6 ± 1.4%, n = 9), CAM treatment attenuated fibrosis area (23.4 ± 3.4%, $p < 0.05$, n = 9) (Figs. 2A and 2B).

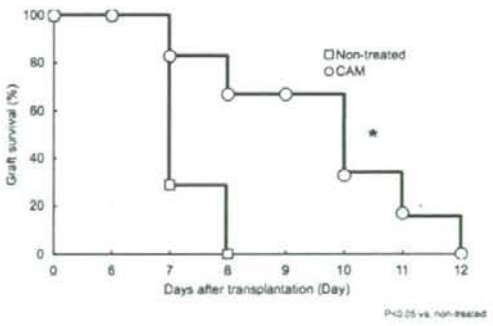


**Figure 1** Survival of Cardiac Allografts

Representative data of graft survival in the full allomismatch combination. Mice treated with clarithromycin (CAM) **(open circles)** showed prolonged cardiac allograft survival in comparison with the nontreated mice **(open squares)**. Nontreated allografts were acutely rejected (7.1 ± 0.2 days, n = 8). However, CAM administration statistically prolonged allograft survival (9.7 ± 0.2 days, n = 8). *$p < 0.05$ versus nontreated group.

JACC Vol. 51, No. 20, 2008
May 20, 2008:1977–85

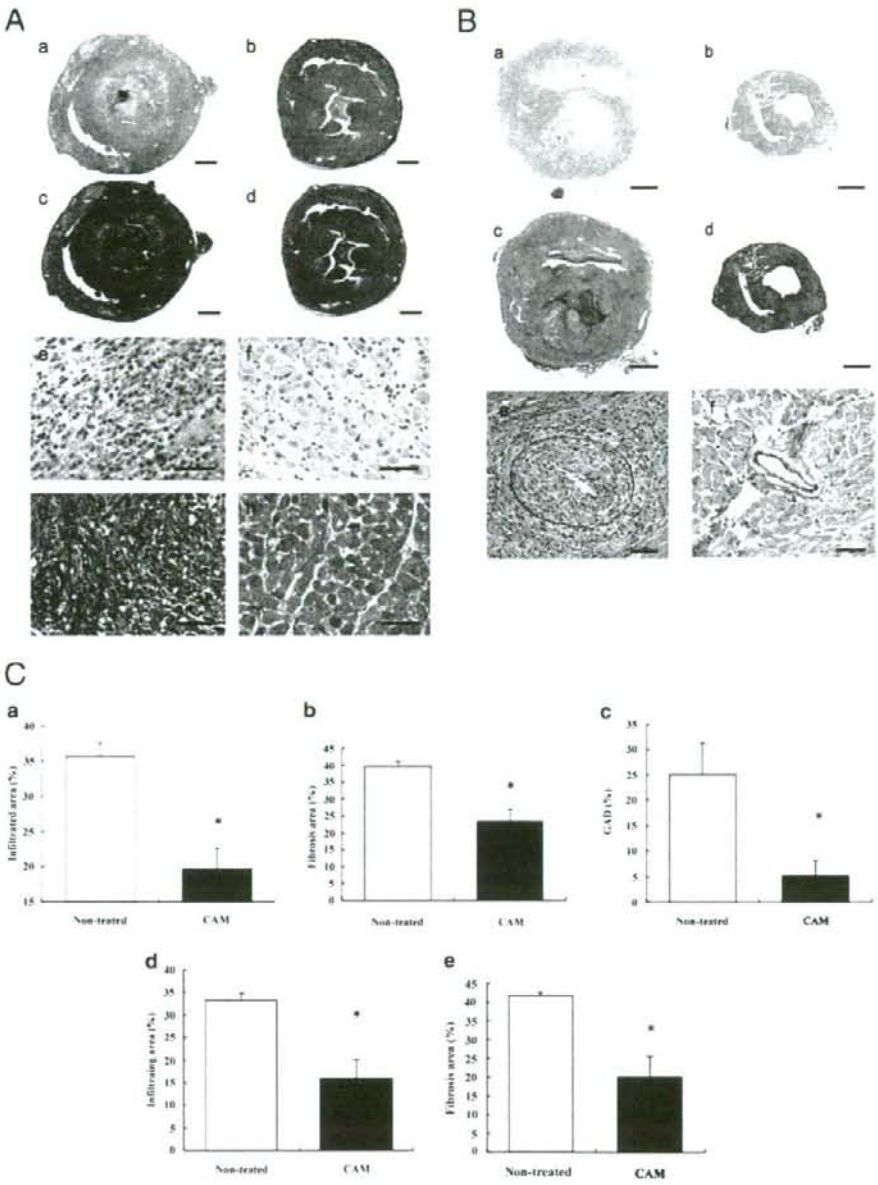


**Figure 2** **Pathological Findings**

Representative light micrographs of allografts from the nontreated group and the clarithromycin (CAM)-treated group. **(A)** Representative pathological findings with hematoxylin and eosin (HE) **(a, b, e, and f)** and Mallory **(c, d, g, and h)** stain in full allomismatch allografts. Although myocardial cell infiltration and fibrosis were observed in nontreatment **(a, c, e, and g)** on day 7, the CAM treatment **(b, d, f, and h)** markedly attenuated them. **Scale bars** = 2 mm **(a to d)** and 50 μm **(e to h)**. **(B)** Representative pathological findings with HE **(a and b)**, Mallory **(c and d)**, and Elastica van Gieson (EvG) **(e and f)** stain in class II mismatch allografts. Although myocardial cell infiltration, fibrosis, and graft arterial disease (GAD) were observed in the nontreated allografts **(a, c, and e)** on day 60, CAM treatment **(b, d, and f)** markedly attenuated them. **Scale bars** = 2 mm **(a to d)** and 25 μm **(e and f)**. **(C)** Quantitative data of cell infiltration **(a)** and fibrosis **(b)** in the full allomismatch combination. Quantitative data of cell infiltration **(d)**, fibrosis **(e)** area, and percentage of neointimal thickening **(c)** in the class II mismatch combination. *$p < 0.05$ versus nontreated group.

In the class II mismatch group, all cardiac allografts kept beating during the observation period and graft function was not different between the groups. Pathologically, severe myocardial cell infiltration (33.3 ± 1.6%, n = 6) and fibrosis (41.8 ± 0.9%, n = 6) were observed in the nontreated group, whereas CAM treatment significantly suppressed infiltration (15.9 ± 4.1%, n = 6, $p < 0.05$ vs. nontreated group) and fibrosis (20.0 ± 5.5%, n = 6, $p < 0.05$ vs. nontreated group) (Figs. 2C and 2D). The heavy neointimal thickening was observed in the coronary arteries of untreated allografts in this combination. However, intimal thickening was attenuated in the CAM-treated group (Fig. 2C [c]).

**Inhibition of inflammatory factors.** Immunohistochemically, enhancement of CD4, CD8, CD11b, NF-κB p65, and ICAM-1 expression was observed in the nontreated allografts of total allomismatch combination. However, CAM treatment markedly attenuated expression of these factors (Fig. 3).

Ribonuclease protection assay was used to examine expression of cytokine mRNA from full allomismatch cardiac grafts on day 7. The mRNA levels of interferon-gamma, IL-6, IL-10, and IL-15 were significantly suppressed in the CAM-treated group compared with those of the nontreated group (Figs. 4A and 4B) (n = 4 each).

**In vivo MMP inhibition.** The MMP activity was markedly enhanced in the infiltrated area in the nontreated full allomismatch group; however, CAM-treated grafts attenuated the MMP activity (Fig. 5A). The MMP inhibitor (+) films show the non–gelatinase-specific activity.

Immunohistochemically, although the nontreated group enhanced the MMP-9 expression in the infiltrating cells, CAM suppressed the expression in total allomismatch combination (Fig. 5B).

**In vitro MMP inhibition.** Serum-starved-J774.1A cells were stimulated with 10 μg/ml IL-1beta recombinant, and after 24 h of stimulation the protein was collected. Although the control group (supplied IL-1beta and dimethyl sulfoxide as a vehicle) markedly enhanced the expression of MMP-9 compared with the native group (nonstimulated), CAM-treated cells significantly suppressed the expression of protein levels. The MMP-2 levels were comparable between the control group and the CAM-treated group (Fig. 6A [a]). The CAM-treated group altered the expression of MMP-9 mRNA but not MMP-2 and TIMP-1 mRNA (Fig. 6A [b]).

Also, SMCs showed that MMP-9 mRNA level was markedly enhanced in the nontreated cells, whereas CAM treatment suppressed the expression of MMP-9 mRNA (Fig. 6B). However, CAM treatment did not alter the mRNA levels of MMP-2 and TIMP-1 compared with the control group.

**Migration and proliferation of SMCs.** In proliferation assay of SMCs, PDGF-BB–stimulated SMCs were significantly proliferated, whereas the CAM treatment (2.0 and 20 μmol/l) attenuated the cell proliferation ($p < 0.05$ vs. control group) (Fig. 7A). The migration assay also showed that enhanced migration into the lower wells was observed in the control group, whereas the CAM-treated group inhibited the migration ($p < 0.05$ vs. control group) (Figs. 7B and 7C).

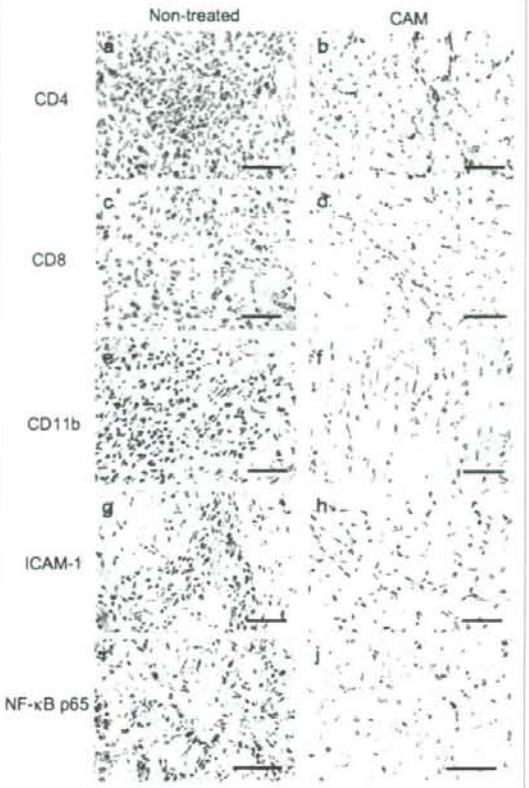


**Figure 3** Immunohistochemistry

Representative immunohistochemistry of allograft from the nontreated group and the clarithromycin (CAM)-treated group. The sections were incubated with CD4 **(a and b)**, CD8 **(c and d)**, CD11b **(e and f)**, intercellular adhesion molecule (ICAM)-1 **(g and h)**, and nuclear factor-κB (NF-κB) p65 **(i and j)**. Although $CD4^+$ **(a)**, $CD8^+$ **(c)**, and $CD11b^+$ **(e)** cells were observed in nontreatment on day 7, CAM treatment markedly attenuated them **(b, d, and f)**. The expression of ICAM-1 **(g)** and NF-κB p65 **(i)** were observed in nontreatment myocardial infiltrating area; however, CAM treatment markedly attenuated them **(h and j)**. **Scale bars** = 50 μm **(a to j)**.

## Discussion

Clarithromycin is not only a potent antibiotic for the treatment of various microbial infections but also has multiple biologic effects. Although the 16-member ring macrolide do not have multiple effects, it is believed that the multiple effects by a macrolide might be characteristic of 14-member ring macrolides (9,23). In this report, we have newly demonstrated that CAM inhibited expression of

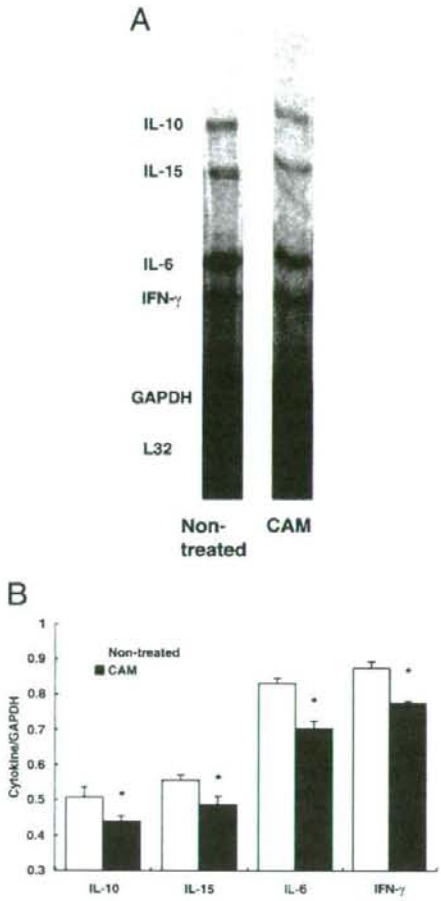


**Figure 4** RPA

**(A)** Representative gels in ribonuclease protection assay (RPA). Messenger ribonucleic acid (mRNA) was isolated from cardiac allografts on day 7. **(B)** The quantitative results. Increase of interleukin (IL)-10, IL-15, IL-6, and interferon (INF) gamma mRNA levels were observed. However, clarithromycin (CAM) treatment markedly attenuated them. *$p < 0.05$ versus nontreated group. GAPDH = glyceraldehyde-3-phosphate dehydrogenase.

MMP-9 and suppressed acute and chronic rejection in murine transplantation models.

Firstly, we demonstrated that CAM suppressed the acute rejection in the MHC total allomismatch combination group. We showed that CAM treatment suppressed MMP-9 and NF-κB activity in this allograft model with zymography and immunohistochemistry. The T lymphocytes and macrophages are a major component of the cellular infiltration in allografts rejection (24,25); they contribute to the development of tissue injury in acute inflammatory reaction (25,26). The MMPs play an important role in cell migration (27) and are involved in the migratory capabilities of inflammatory cells such as T-cells (6). The MMP-9 is known to be especially important in inflammation, and the gelatinase have been shown to play a critical role in the process of the infiltration in inflamed tissues (28). We demonstrated that CAM attenuated $CD4^+$, $CD8^+$, and $CD11b^+$ cell infiltration, altered the expression of inflammatory cytokines, and consequently decreased the infiltration and fibrosis compared with the control group in cardiac allografts. It has previously been reported that CAM inhibits the activation of NF-κB and activator protein-1 (4,5). The interaction between ICAM-1 and the receptor lymphocyte function-associated antigen-1 affects both alloantigen specific and nonspecific phases of graft destruction after heart transplantation. The ICAM-1 is regulated by NF-κB, which is a key transcription factor of inflammation or immunosuppression (29). At this point, there has been no report to compare the immunological effects in transplantation between CAM and immunosuppressive agents directly in vivo. However, there was a report to clarify the difference between CAM

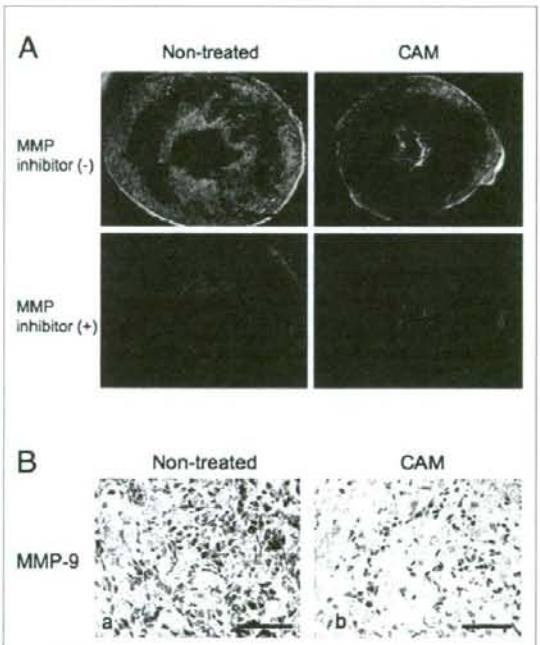


**Figure 5** MMP Activity

**(A)** Representative results of gelatinase's activity. In the matrix metalloproteinases (MMPs) inhibitor (−) group, gelatinase's activity was generally observed in the myocardial infiltrating area in full allografts **(a)**. However, clarithromycin (CAM) treatment markedly attenuated gelatinase's activity **(b)**. The MMPs inhibitor (+) films show the non–gelatinase-specific activity **(c and d)**. **Scale bars** = 4 mm **(a to d)**. **(B)** Representative results of immunohistochemistry. Although expression of MMP-9 was observed in the infiltrating cells in nontreatment allografts **(a)**, CAM treatment suppressed the expression **(b)**. **Scale bars** = 50 μm **(a and b)**.

and immunosuppressive drugs such as FK506 in vitro (30). The article demonstrated that CAM could modify T-cell proliferation and IL-2 production. This showed that CAM has similar effects on FK506. However, they also showed that combined treatment with CAM (1.6 to 40 μg/ml) and FK506 (0.0001 to 0.001 μg/ml) resulted in an additional inhibition of T-cell proliferation. These results suggest that pharmacokinetics is significantly different, and there are different immunological receptors

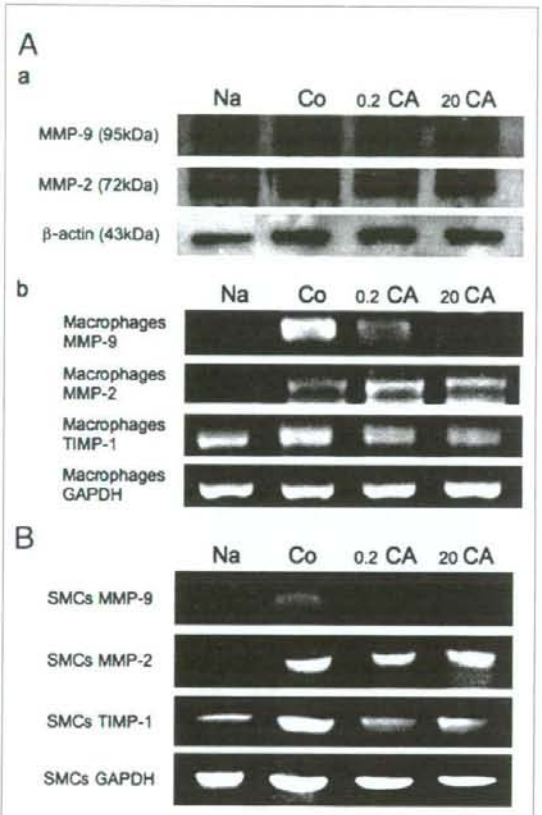


**Figure 6** In Vitro MMP-9 Inhibition

**(A)** Representative Western blot data detecting the expression of matrix metalloproteinases (MMP)-9 and -2 proteins in macrophages **(a)**. The control group (Co) markedly enhanced the expression of MMP-9 compared with native (Na). The 0.2- and 20-μmol/l clarithromycin (CAM) treatment (0.2 CA and 20 CA) altered the MMP-9 protein levels compared with the control group. However, MMP-2 expression was not altered by CAM treatment. **(b)** Representative gels showed the expression of MMP-9, MMP-2, and tissue inhibitor metalloproteinase (TIMP)-1 messenger ribonucleic acid (mRNA) levels by reverse transcriptase-polymerase chain reaction (RT-PCR). The CAM treatment altered the expression of MMP-9 but not MMP-2 and TIMP-1. The treatment of 20 μmol/l CAM inhibited expression of MMP-9 more effectively than that of 0.2 μmol/l. **(B)** Representative RT-PCR data detecting the expression of MMP-9, MMP-2, and TIMP-1 mRNA in the smooth muscle cells (SMCs). The control group markedly expressed MMP-9, and CAM treatment inhibited the expression of MMP-9 mRNA levels. The CAM treatment did not alter the MMP-2 and TIMP-1 expression. GAPDH = glyceraldehyde-3-phosphate dehydrogenase.

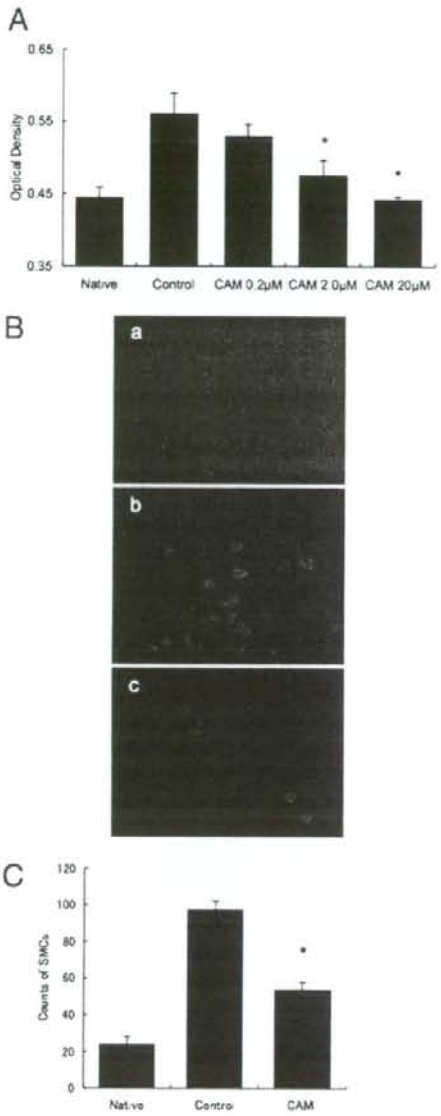


**Figure 7** Proliferation and Migration Assays

**(A)** Quantitative data of proliferation assay. Markedly increase proliferation of the smooth muscle cells (SMCs) was observed by stimulation of PDGF-BB (Biosource International, Camarillo, California) compared with those of the native group. The 0.2-μmol/l clarithromycin (CAM) treatment did not significantly inhibit the cell proliferation, whereas 2.0- and 20-μmol/l CAM treatment significantly inhibited the proliferation compared with the control group. *$p < 0.05$ versus control group. **(B)** Representative light micrographs of migration assay. Although the SMCs markedly migrated to a lower well by the stimulation of PDGF-BB **(b)** compared with those in the native group **(a)**, CAM (20 μmol/l) treatment **(c)** significantly suppressed the SMC migration. **(C)** The quantitative data of migration assay. Counts of SMCs in a lower well significantly decreased in CAM-treatment group compared with the control group. *$p < 0.05$ versus control group.

JACC Vol. 51, No. 20, 2008
May 20, 2008:1977–85

or signal cascades between CAM and FK506. Further studies would be needed to compare the immunological effects between CAM and conservative immunosuppressive agents.

Secondly, we demonstrated that CAM inhibited the development of graft arterial disease (GAD) formation in the MHC class II mismatch combination. Although GAD ultimately culminates in vascular stenosis and ischemic graft failure, the infallible cure and prevention measures are still unknown. Therefore, it is noteworthy that CAM, which has been broadly used in clinical settings, can suppress the development of GAD that could not be prevented with conservative therapies. Chronic MHC class II mismatch allo-responses induce inflammatory and vascular wall cells to secrete growth factors that promote SMC intimal recruitment, proliferation, and matrix synthesis (31,32). Whereas pro-MMP-2 is basally produced by unstimulated SMCs in vitro, MMP-9 are produced after cytokine stimulation (33); MMP-9 is known to be required for SMC migration (34) and contributing to the intimal thickening hyperplasia of vascular lesion (14,35). The TIMP-1 is known as a natural inhibitor of MMP-9, and inhibition of MMP-9 by TIMP-1 is shown to decrease SMC migration and subsequent neointimal hyperplasia in the vascular injury model (36). The NF-$\kappa$B was well known as the regulator of the MMP-9 and -2; however, our data showed that CAM attenuated the expression of MMP-9 but not MMP-2 by Western blot and RT-PCR in macrophages and SMCs. The results might indicate indirect inhibition of NF-$\kappa$B activity by CAM treatment. In addition, our data showed that CAM attenuated the expression of MMP-9 without the alternation of TIMP-1; CAM might have an effect that directly inhibits the expression of MMP-9 mRNA without TIMP-1 activation. Previously, other investigators reported that erythromycin, one of the 14-member ring macrolides, suppressed the production of both MMP-9 and -2 in vitro (9,37). Interestingly, we demonstrated that CAM suppressed the production of MMP-9 but not MMP-2 in this report. Our data indicate that CAM has the potential to be a selective MMP-9 inhibitor. However, the detailed mechanism between CAM and MMP-9 has not yet been elucidated. Further investigation is needed. Although CAM inhibited GAD development and myocardial remodeling, graft function was not different between the groups in the MHC class II mismatch combination. Because murine graft function was evaluated by palpation in this study, this method might lack enough sensitivity to quantitatively evaluate graft function. An echocardiogram would be useful to analyze the function when it is applicable in future.

The dosage of CAM we used in this study (100 mg/kg/day) was approximately 10 times as large as the clinical dosage (10 to 20 mg/kg/day). Pharmacokinetics of CAM was different between mice and humans, as previously reported, and the various doses (5 to 600 mg/kg/day) of CAM could be used for murine examinations (16,17). Thus, we selected the dose for mice. However, further studies would be needed to determine an optimal dose-effect relationship.

We demonstrated for the first time that CAM suppressed myocardial inflammation and fibrosis through the attenuation of the inflammatory cell migration and myocardial cell infiltration by inhibition of MMP-9 activity, which resulted in suppression of acute cardiac rejection. In chronic rejection, CAM suppressed GAD development through the suppression of SMC proliferation and migration by MMP-9 inhibition. Although we focused on MMP-9 in this study, our results could not show direct evidence that CAM inhibition of MMP-9 was the primary effect of the drug. Therefore, further investigation would be needed to determine the importance of other factors that are modified by CAM.

In conclusion, CAM plays a significant role in the prevention of acute and chronic rejection through the inhibition of MMP-9 activity. Clarithromycin might be used in the suppression of transplant rejection and cardiovascular and other inflammatory diseases in clinical settings.

**Acknowledgments**

The authors thank Ms. Noriko Tamura and Ms. Yasuko Matsuda for their excellent technical assistance.

**Reprint requests and correspondence:** Dr. Jun-ichi Suzuki, Department of Cardiovascular Medicine, Tokyo Medical and Dental University, 1-5-45 Yushima, Bunkyo-ku, Tokyo 113-8519 Japan. E-mail: jsuzuki.cvm@tmd.ac.jp.

## REFERENCES

1. Isobe M, Yagita H, Okumura K, Ihara A. Specific acceptance of cardiac allograft after treatment with antibodies to ICAM-1 and LFA-1. Science 1992;255:1125–7.
2. Suzuki J, Isobe M, Aikawa M, et al. Nonmuscle and smooth muscle myosin heavy chain expression in rejected cardiac allografts. A study in rat and monkey models. Circulation 1996;94:1118–24.
3. Taylor DO, Edwards LB, Boucek MM, et al. Registry of the International Society for Heart and Lung Transplantation: twenty-second official adult heart transplant report—2005. J Heart Lung Transplant 2005;24:945–55.
4. Kikuchi T, Hagiwara K, Honda Y, et al. Clarithromycin suppresses lipopolysaccharide-induced interleukin-8 production by human monocytes through AP-1 and NF-kappa B transcription factors. J Antimicrob Chemother 2002;49:745–55.
5. Abe S, Nakamura H, Inoue S, et al. Interleukin-8 gene repression by clarithromycin is mediated by the activator protein-1 binding site in human bronchial epithelial cells. Am J Respir Cell Mol Biol 2000;22:51–60.
6. Leppert D, Waubant E, Galardy R, Bunnett NW, Hauser SL. T cell gelatinases mediate basement membrane transmigration in vitro. J Immunol 1995;154:4379–89.
7. Xia M, Leppert D, Hauser SL, et al. Stimulus specificity of matrix metalloproteinase dependence of human T cell migration through a model basement membrane. J Immunol 1996;156:160–7.

8. Hibbs MS, Hoidal JR, Kang AH. Expression of a metalloproteinase that degrades native type V collagen and denatured collagens by cultured human alveolar macrophages. J Clin Invest 1987;80:1644–50.
9. Hashimoto N, Kawabe T, Hara T, et al. Effect of erythromycin on matrix metalloproteinase-9 and cell migration. J Lab Clin Med 2001;137:176–83.
10. Ermolli M, Schumacher M, Lods N, Hammoud M, Marti HP. Differential expression of MMP-2/MMP-9 and potential benefit of an MMP inhibitor in experimental acute kidney allograft rejection. Transpl Immunol 2003;11:137–45.
11. Suzuki J, Isobe M, Kawauchi M, Endoh M, Amano J, Takamoto S. Altered expression of matrix metalloproteinases and tissue inhibitors of metalloproteinases in acutely rejected myocardium and coronary arteriosclerosis in cardiac allografts of nonhuman primates. Transpl Int 2000;13:106–13.
12. Yamani MH, Starling RC, Young JB, et al. Acute vascular rejection is associated with up-regulation of vitronectin receptor (alphavbeta3), increased expression of tissue factor, and activation of the extracellular matrix metalloproteinase induction system. J Heart Lung Transplant 2002;21:983–9.
13. Cho A, Reidy MA. Matrix metalloproteinase-9 is necessary for the regulation of smooth muscle cell replication and migration after arterial injury. Circ Res 2002;91:845–51.
14. Mason DP, Kenagy RD, Hasenstab D, et al. Matrix metalloproteinase-9 overexpression enhances vascular smooth muscle cell migration and alters remodeling in the injured rat carotid artery. Circ Res 1999;85:1179–85.
15. Suzuki J, Ogawa M, Sagesaka YM, Isobe M. Tea catechins attenuate ventricular remodeling and graft arterial diseases in murine cardiac allografts. Cardiovasc Res 2006;69:272–9.
16. Tessier PR, Kim MK, Zhou W, et al. Pharmacodynamic assessment of clarithromycin in a murine model of pneumococcal pneumonia. Antimicrob Agents Chemother 2002;46:1425–34.
17. Vallee E, Azoulay-Dupuis E, Swanson R, Bergogne-Berezin E, Pocidalo JJ. Individual and combined activities of clarithromycin and its 14-hydroxy metabolite in a murine model of Haemophilus influenzae infection. J Antimicrob Chemother 1991;27 Suppl A:31–41.
18. Suzuki J, Koga N, Kosuge H, et al. Pitavastatin suppresses acute and chronic rejection in murine cardiac allografts. Transplantation 2007; 83:1093–7.
19. Kosuge H, Haraguchi G, Koga N, Maejima Y, Suzuki J, Isobe M. Pioglitazone prevents acute and chronic cardiac allograft rejection. Circulation 2006;113:2613–22.
20. Wright JW, Brown TE, Harding JW. Inhibition of hippocampal matrix metalloproteinase-3 and -9 disrupts spatial memory. Neural Plast 2007. [E-pub ahead of print].
21. Suzuki J, Ogawa M, Futamatsu H, Kosuge H, Tanaka H, Isobe M. A cyclooxygenase-2 inhibitor alters Th1/Th2 cytokine balance and suppresses autoimmune myocarditis in rats. J Mol Cell Cardiol 2006;40: 688–95.
22. Kuzuya M, Kanda S, Sasaki T, et al. Deficiency of gelatinase a suppresses smooth muscle cell invasion and development of experimental intimal hyperplasia. Circulation 2003;108:1375–81.
23. Kanai K, Asano K, Hisamitsu T, Suzaki H. Suppression of matrix metalloproteinase production from nasal fibroblasts by macrolide antibiotics in vitro. Eur Respir J 2004;23:671–8.
24. Ascher NL, Ferguson RM, Hoffman R, Simmons RL. Partial characterization of cytotoxic cells infiltrating sponge matrix allografts. Transplantation 1979;27:254–9.
25. Isobe M, Suzuki J. New approaches to the management of acute and chronic cardiac allograft rejection. Jpn Circ J 1998;62:315–27.
26. Mazzarella G, Petillo O, Margarucci S, Calabrese C, Peluso G. Role of monocyte/macrophage population in immune response. Monaldi Arch Chest Dis 1998;53:92–6.
27. Giannelli G, Falk-Marzillier J, Schiraldi O, Stetler-Stevenson WG, Quaranta V. Induction of cell migration by matrix metalloprotease-2 cleavage of laminin-5. Science 1997;277:225–8.
28. Dubois B, Masure S, Hurtenbach U, et al. Resistance of young gelatinase B-deficient mice to experimental autoimmune encephalomyelitis and necrotizing tail lesions. J Clin Invest 1999;104:1507–15.
29. Li Q, Verma IM. NF-kappaB regulation in the immune system. Nat Rev Immunol 2002;2:725–34.
30. Morikawa K, Oseko F, Morikawa S, Iwamoto K. Immunomodulatory effects of three macrolides, midecamycin acetate, josamycin, and clarithromycin, on human T-lymphocyte function in vitro. Antimicrob Agents Chemother 1994;38:2643–7.
31. Hayry P. Chronic rejection: an update on the mechanism. Transplant Proc 1998;30:3993–5.
32. Libby P, Tanaka H. The pathogenesis of coronary arteriosclerosis ("chronic rejection") in transplanted hearts. Clin Transplant 1994;8:313–8.
33. Galis ZS, Muszynski M, Sukhova GK, et al. Cytokine-stimulated human vascular smooth muscle cells synthesize a complement of enzymes required for extracellular matrix digestion. Circ Res 1994;75: 181–9.
34. Kenagy RD, Hart CE, Stetler-Stevenson WG, Clowes AW. Primate smooth muscle cell migration from aortic explants is mediated by endogenous platelet-derived growth factor and basic fibroblast growth factor acting through matrix metalloproteinases 2 and 9. Circulation 1997;96:3555–60.
35. de Smet BJ, de Kleijn D, Hanemaaijer R, et al. Metalloproteinase inhibition reduces constrictive arterial remodeling after balloon angioplasty: a study in the atherosclerotic Yucatan micropig. Circulation 2000;101:2962–7.
36. Lijnen HR, Soloway P, Collen D. Tissue inhibitor of matrix metalloproteinases-1 impairs arterial neointima formation after vascular injury in mice. Circ Res 1999;85:1186–91.
37. Guo H, Lee JD, Yue H, et al. Effect of erythromycin on homocysteine-induced extracellular matrix metalloproteinase-2 production in cultured rat vascular smooth muscle cells. Indian J Med Res 2005;121:764–70.

Clinical

www.clinsci.org

Clinical Science (2008) 114, 431–440 (Printed in Great Britain) doi:10.1042/CS20070179



# A novel β-myosin heavy chain gene mutation, p.Met531Arg, identified in isolated left ventricular non-compaction in humans, results in left ventricular hypertrophy that progresses to dilation in a mouse model

**Tomoya KANEDA*[1], Chie NARUSE†[1], Atsuhiro KAWASHIMA‡, Noboru FUJINO*, Toru OSHIMA§, Masanobu NAMURA‖, Shinichi NUNODA¶, Sumio MORI**, Tetsuo KONNO*, Hidekazu INO*, Masakazu YAMAGISHI* and Masahide ASANO†**

*Division of Cardiovascular Medicine, Kanazawa University Graduate School of Medicine, Kanazawa, Ishikawa, Japan, †Division of Transgenic Animal Science, Advanced Science Research Center, Kanazawa University, Kanazawa, Ishikawa, Japan, ‡Division of Pathology, National Hospital Organization, Kanazawa Medical Center, Kanazawa, Ishikawa, Japan, §Division of Environmental Science, Forensic and Social Environmental Medicine, Kanazawa University Graduate School of Medicine, Kanazawa, Ishikawa, Japan, ‖Division of Cardiology, Kanazawa Cardiovascular Hospital, Kanazawa, Ishikawa, Japan, ¶Department of Internal Medicine, Tokyo Women's Medical University Medical Center East, Tokyo, Japan, and **Division of Cardiology, Hoju Memorial Hospital, Ishikawa, Japan

## ABSTRACT

Mutations in the βMHC (β-myosin heavy chain), a sarcomeric protein are responsible for hypertrophic and dilated cardiomyopathy. However, the mechanisms whereby distinct mutations in the βMHC gene cause two kinds of cardiomyopathy are still unclear. In the present study we report a novel βMHC mutation found in a patient with isolated LVNC [LV (left ventricular) non-compaction] and the phenotype of a mouse mutant model carrying the same mutation. To find the mutation responsible, we searched for genomic mutations in 99 unrelated probands with dilated cardiomyopathy and five probands with isolated LVNC, and identified a p.Met531Arg mutation in βMHC in a 13-year-old girl with isolated LVNC. Next, we generated six lines of transgenic mice carrying a p.Met532Arg mutant αMHC gene, which was identical with the p.Met531Arg mutation in the human βMHC. Among these, two lines with strong expression of the mutant αMHC gene were chosen for further studies. Although they did not exhibit the features characteristic of LVNC, approx. 50% and 70% of transgenic mice in each line displayed LVH (LV hypertrophy) by 2–3 months of age. Furthermore, LVD (LV dilation) developed in approx. 25% of transgenic mice by 18 months of age, demonstrating biphasic changes in LV wall thickness. The present study supports the idea that common mechanisms may be involved in LVH and LVD. The novel mouse model generated can provide important information for the understanding of the pathological processes and aetiology of cardiac dilation in humans.

**Key words:** cardiomyopathy, left ventricular non-compaction, mutation, myosin heavy chain, transgenic mouse.

**Abbreviations:** DCM, dilated cardiomyopathy; FS, fractional shortening; GAPDH, glyceraldehyde-3-phosphate dehydrogenase; gDNA, genomic DNA; H and E, Haemotoxylin and Eosin; HCM, hypertrophic cardiomyopathy; IVST, interventricular septal thickness; LV, left ventricular; LVD, LV dilation; LVEDD, LV end-diastolic diameter; LVESD, LV end-systolic diameter; LVEF, LV ejection fraction; LVH, LV hypertrophy; LVNC, LV non-compaction; MHC, myosin heavy chain; PWT, posterior wall thickness; RT, reverse transcription; SSCP, single-strand conformational polymorphism.

[1] These authors contributed equally to this study.

**Correspondence:** Dr Tomoya Kaneda (email tomoya1311@yahoo.co.jp).